# Strained Ruthenium Complexes Bearing Tridentate Guanidine-Derived Ligands

Eden-Taylor Wilkinson, Fernando Viguri, Ricardo Rodríguez, José A. López, Pilar García-Orduña, Fernando J. Lahoz, Pilar Lamata* and Daniel Carmona*

Instituto de Síntesis Química y Catálisis Homogénea (ISQCH), CSIC-Universidad de Zaragoza, Departamento de Química Inorgánica, Pedro Cerbuna 12, 50009 Zaragoza, Spain, e-mail: plamata@unizar.es, dcarmona@unizar.es

Dedicated to *E. Peter Kündig*, Honorary Professor of Organic Chemistry, on the occasion of his 75th birthday

The dimer [{($\eta^6$-*p*-cymene)RuCl}$_2$($\mu$-Cl)$_2$] (cymene = MeC$_6$H$_4$*i*Pr) reacts with *N*,*N'*-bis(*p*-Tolyl)-*N''*-(2-pyridinylmethyl)guanidine (**H$_2$L1**) and *N*,*N'*-bis(*p*-Tolyl)-*N''*-(2-diphenylphosphanoethyl)guanidine (**H$_2$L2**), in the presence of NaSbF$_6$, giving rise to chlorido compounds of formula [($\eta^6$-*p*-cymene)RuCl(**H$_2$L**)][SbF$_6$] (**H$_2$L** = **H$_2$L1** (**1**), **H$_2$L2** (**2**)) in which the guanidine ligand adopts a $\kappa^2$ chelate coordination mode. The related ligand (*S*)-*N*,*N'*-bis(*p*-Tolyl)-*N''*-(1-isopropyl, 2-diphenylphosphano ethyl)guanidine (**H$_2$L3**) affords mixtures of the corresponding chlorido compound [($\eta^6$-*p*-cymene)RuCl(**H$_2$L3**)][SbF$_6$] (**3**) together with the complexes [($\eta^6$-*p*-cymene)RuCl$_2$(**H$_3$L3**)][SbF$_6$] (**4**) and [($\eta^6$-*p*-cymene)Ru($\kappa^3$*N*,*N'*,*P*-**HL3**)][SbF$_6$] (**10**) which contain phosphano-guanidinium and phosphano-guanidinato ions acting as monodentate and tridentate ligand, respectively. Compounds **1**, **2** and mixture of **3**/**4**/**10** react with AgSbF$_6$ rendering the cationic aqua-complexes [($\eta^6$-*p*-cymene)Ru(**H$_2$L**)(OH$_2$)][SbF$_6$]$_2$ (**H$_2$L** = **H$_2$L1** (**5**), **H$_2$L2** (**6**), **H$_2$L3** (**7**)). These aqua-complexes exhibit a temperature dependent fluxional process in solution. Experimental NMR studies and DFT theoretical calculations on complex **6** suggest that the process involve the exchange between two rotamers around one of the C−N guanidine bonds. Treatment of **5-7** with NaHCO$_3$ renders the complexes [($\eta^6$-*p*-cymene)Ru($\kappa^3$*N*,*N'*,*N''*-**HL1**)][SbF$_6$] (**8**) and [($\eta^6$-*p*-cymene)Ru($\kappa^3$*N*,*N'*,*P*-**HL**)][SbF$_6$] (**HL** = **HL2** (**9**), **HL3** (**10**)), respectively, in which the **HL** ligand adopts a *fac* $\kappa^3$ coordination mode. The new complexes have been characterised by analytical and spectroscopic means, including the determination of the crystal structures of the compounds **1**, **2**, **5**, **9** and **10**, by X-ray diffractometric methods.

**Keywords**: guanidine-derived ligands, half-sandwich complexes, ruthenium, strained metallacycles.

## Introduction

Guanidines have the capability to stabilise metallic ions by making use of their ability to act as neutral or ionic ligands in a variety of coordination modes.[1-10] It should be noted that the combination of nitrogen-based functionalities that guanidines present allows the incorporation of a variety of substituents with coordination capacity. In this way, the potential of the chemistry of the compounds involved is favourably affected by the properties associated to the newly incorporated groups. As a result, guanidines and guanidine-based metallic compounds have found important applications in fields such as catalysis,[1,4,11-15] materials science[3,4,13,16] or supramolecular chemistry.[3,17,18]

On the other hand, the last years have witnessed the development of the chemistry of a new type of species called frustrated Lewis pair (FLP). FLP is an intra- or inter-molecular system in which a Lewis acid and a Lewis base do not yield the classical Lewis acid/base adduct because of steric and/or electronic factors.[19] The interest of this type of compound lies in the novel cooperative reactivity between its acidic and basic components that encompasses a variety of stoichiometric and catalytic molecular activation processes.[20-32] In the first reported examples, the roles of Lewis acid and Lewis base were played by main group elements but the potential of these systems strongly increased with the incorporation of components based on transition metals resulting in the so-called transition-metal frustrated Lewis pairs (TMFLPs).[33-37]

In this context, we have recently communicated the preparation of the rhodium-guanidinato complex **I** (Scheme 1**A**) in which one of the guanidinate nitrogens bears an ethylen-diphenylphosphane substituent. Complex **I** behaves as a "dormant" frustrated Lewis pair (FLP)[38-40] able to reversibly activate polar, H−OH, and nonpolar, H−H, bonds showing FLP mechanisms.[41] The FLP behaviour of complex **I** can be realised by

analysing its structural features. Thus, the Cp* ligand, formally occupying three *fac* coordination positions, obliges the tridentate phosphano-guanidinato ligand to adopt also a *fac* coordination mode. This coordination forces the central nitrogen atom ($N^1$) to embrace an $sp^3$ hybridization. Under these conditions, the Rh−$N^1$−C−$N^2$ four-membered cycle hold up a strong ring strain that can be relaxed by breaking the Rh−$N^2$ bond, as it is shown in Scheme 1**B**, giving rise to an active FLP species. Notably, the coordinated phosphano arm contributes to maintain the molecular entity of the compound avoiding undesired side reactions.

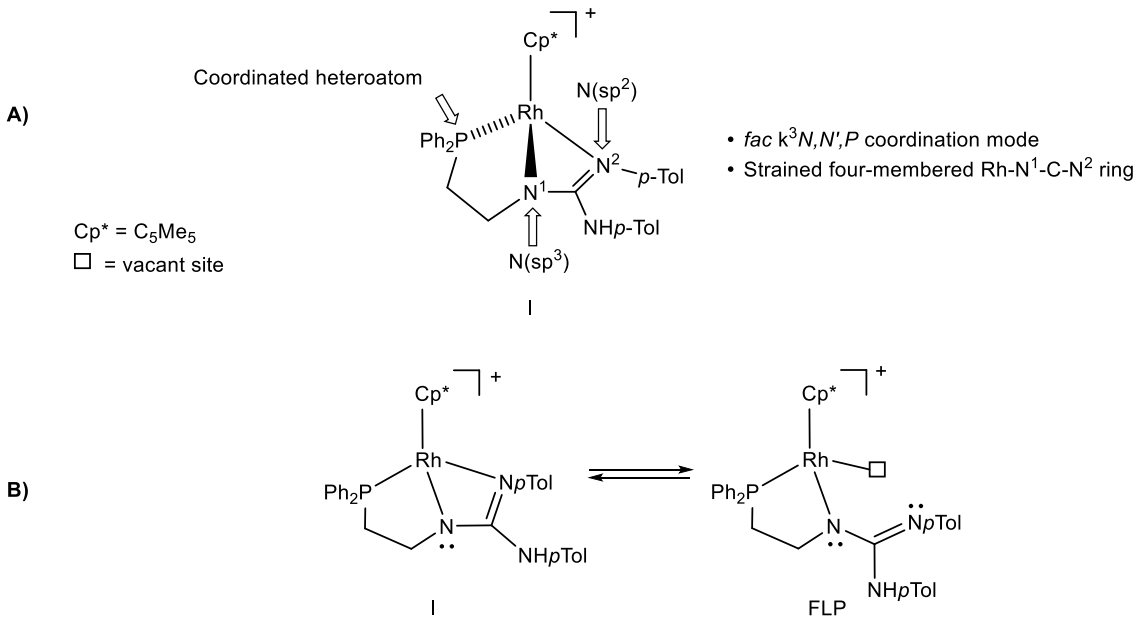


**Scheme 1**. Dormant FLP rhodium-guanidinato complex **I** and equilibrium that gives rise to the active FLP species.

Taking into account that $Ru^{2+}$ and $Rh^{3+}$ are isoelectronic, we anticipated that functionalised guanidinato ligands could render (arene)Ru(II) complexes with structural and chemical features comparable to those of the Cp*Rh(III) complex **I**, and therefore, would generate potentially active TMFLP species based on ruthenium.

In this paper, we report the preparation and characterisation of (*p*-cymene)Ru(II) (cymene = $MeC_6H_4iPr$) complexes bearing as ligands pyridinyl-guanidine **$H_2$L1** and the

phosphano-guanidines **$H_2$L2** and **$H_2$L3** (Scheme 2) in an attempt to prepare half-sandwich ruthenium compounds able to show FLP reactivity.

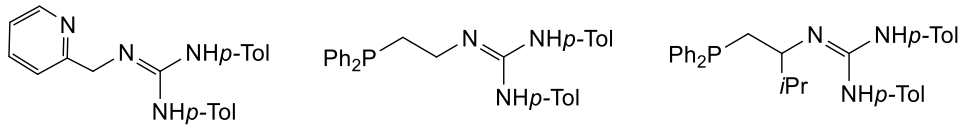


**$H_2$L1** **$H_2$L2** **$H_2$L3**

**Scheme 2.** Pyridinyl- and phosphano-guanidine ligands employed.

## Results and Discussion

### Synthesis of the ligands

The preparation of the ligands **H₂L1** and **H₂L2** has been previously reported.[42] The new phosphano-guanidine ligand **H₂L3** has been prepared by reacting 1,3-di(*p*-tolyl)carbodiimide with (*S*)-1-(diphenylphosphino)-2-amino-3-methylbutane (Scheme 3) in dry THF following a similar procedure than that reported for **H₂L2** (see Experimental Section).[43]

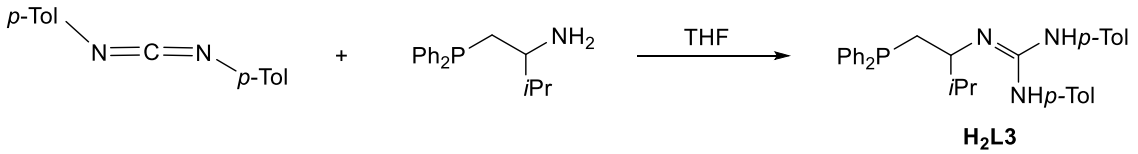


**Scheme 3**. Preparation of the ligand **H₂L3**.

### Synthesis of the chlorido complexes [($\eta^6$-*p*-cymene)RuCl(H₂L)][SbF₆] (H₂L = H₂L1 (1), H₂L2 (2))

Methanolic suspensions of the ruthenium dimer [{($\eta^6$-*p*-cymene)RuCl}$_2$($\mu$-Cl)$_2$][44] react with **H₂L1** or **H₂L2** in the presence of $NaSbF_6$ affording the cationic complexes [($\eta^6$-*p*-cymene)RuCl(**H₂L**)][$SbF_6$] (**H₂L** = **H₂L1** (**1**), **H₂L2** (**2**)) in good isolated yield (Scheme 4).

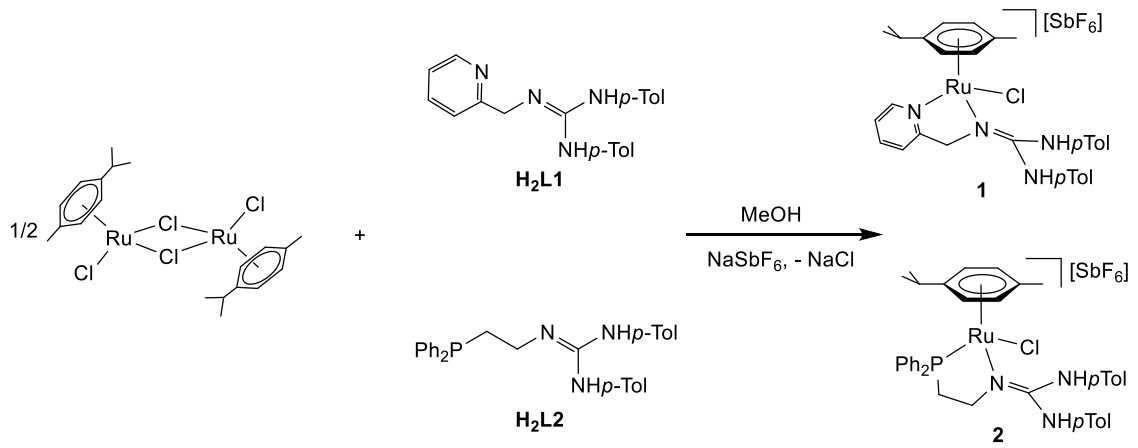

**Scheme 4**. Preparation of the chlorido complexes **1** and **2**.

The complexes were characterized by analytical and spectroscopic means (see Experimental Section). Assignment of the NMR signals was verified by two-dimensional homonuclear and heteronuclear correlations. The strong deshielding of the $H_6$ proton of the pyridine moiety in complex **1** −from 8.25 (free ligand) to 8.93 ppm− and that of the phosphorus nucleus in complex **2** −about 75 ppm− indicate that the pyridine nitrogen and the diphenylphosphane phosphorus atoms are coordinated to the metal in complexes **1** and **2**, respectively.

Chelate $\kappa^2$*N,N'* and $\kappa^2$*N,P* coordination modes of the **$H_2$L** ligand give rise to five-membered metallacycles (see Scheme 4) and render the ruthenium atom a stereogenic centre and the methylene groups diastereotopic. As a consequence, the methylene groups of both complexes ($CH_2$−N (**1**) and P−$CH_2$−$CH_2$−N (**2**)), are asynchronous (see Experimental Section). Indeed, the presence or absence of NOE interactions with the *p*-cymene protons allows the discrimination between *pro-R* and *pro-S* protons within each methylene pair.

The solid state structure of both complexes was determined by X-ray diffraction means. Both compounds crystallise as racemate in the $P\bar{1}$ (complex **1**) and $P2_1/c$ (complex **2**) space groups. In the asymmetric unit of complex **2**, the structural analysis revealed the presence of two crystallographically independent, but chemically equivalent, molecules. Views of the cation of the $S_{Ru}$-**1** complex (priority order: *p*-cymene > Cl > N(2) > N(1)) and of the cation of the $R_{Ru}$-**2** complex (priority order: *p*-cymene > Cl > P(1) > N(1))[45] are depicted in Fig. 1 and relevant structural characteristics of the cations are summarised in Table 1.

Both complexes exhibit the so-called "three-legged piano-stool" geometry. An $\eta^6$-*p*-cymene group occupies three *fac* positions and the corresponding ligand, **H$_2$L1** (**1**) or **H$_2$L2** (**2**), occupies two coordination sites adopting a $\kappa^2 N,N'$ or $\kappa^2 N,P$ coordination mode.

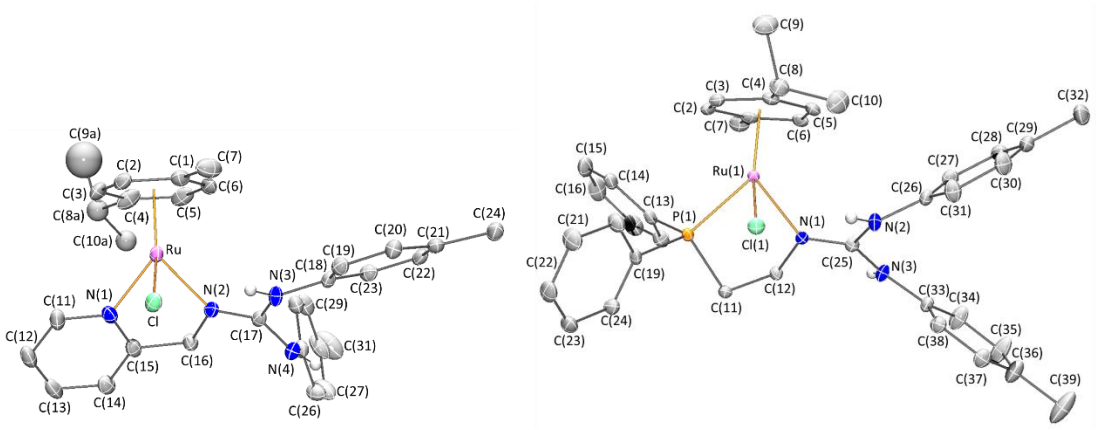


**Figure 1**. Molecular structure of the cations of complexes **1** and one of the crystallographically independent molecules of **2**. For clarity all the hydrogen atoms are omitted, except the NH protons.

**Table 1**. Selected bond lengths (Å) and angles (º) for complexes **1** and **2**.

| | **1** | | **2 (molecule a)**[b] | **2 (molecule b)**[b] |
|---|---|---|---|---|
| Ru-Cl | 2.4263(8) | Ru(1)-Cl(1) | 2.4042(5) | 2.3969(5) |
| Ru-N(1) | 2.090(3) | Ru(1)-P(1) | 2.3265(5) | 2.3098(5) |
| Ru-N(2) | 2.105(3) | Ru(1)-N(1) | 2.1359(16) | 2.1268(17) |
| Ru-Ct[a] | 1.6846(1) | Ru(1)-Ct(1)[a] | 1.7166(1) | 1.7174(1) |
| Cl-Ru-N(1) | 85.60(8) | Cl(1)-Ru(1)-P(1) | 86.125(18) | 86.284(19) |
| Cl-Ru-N(2) | 87.71(8) | Cl(1)-Ru(1)-N(1) | 85.26(5) | 84.66(5) |
| Cl-Ru-Ct[a] | 127.32(1) | Cl(1)-Ru(1)-Ct(1)[a] | 127.29(1) | 126.45(1) |
| N(1)-Ru-N(2) | 76.96(11) | P(1)-Ru(1)-N(1) | 81.37(5) | 81.82(5) |
| N(1)-Ru-Ct[a] | 131.19(1) | P(1)-Ru(1)-Ct(1)[a] | 131.50(1) | 131.48(1) |
| N(2)-Ru-Ct[a] | 130.82(1) | N(1)-Ru(1)-Ct(1)[a] | 128.90(1) | 129.78(1) |
| N(2)-C(16) | 1.465(4) | N(1)-C(12) | 1.476(2) | 1.478(3) |
| N(2)-C(17) | 1.310(4) | N(1)-C(25) | 1.314(3) | 1.308(3) |
| N(3)-C(17) | 1.361(4) | N(2)-C(25) | 1.368(3) | 1.369(3) |
| N(4)-C(17) | 1.364(4) | N(3)-C(25) | 1.366(3) | 1.380(3) |
| $\sum \widehat{C(17)}$[c] | 359.9(5) | $\sum \widehat{C(25)}$[c] | 360.0(3) | 360.0(3) |
| $\sum \widehat{N(2)}$[c] | 359.8(4) | $\sum \widehat{N(1)}$[c] | 360.0(2) | 359.9(2) |
| $\sum \widehat{N(3)}$[c] | 360(3) | $\sum \widehat{N(2)}$[c] | 359(2) | 360(2) |
| $\sum \widehat{N(4)}$[c] | 356(4) | $\sum \widehat{N(3)}$[c] | 360(2) | 359(2) |

[a] Ct stands for the centroid of the *p*-cymene ligand. [b] The asymmetric unit of complex **2** contains two crystallographically independent molecules.[c] $\sum \hat{C}$ and $\sum \hat{N}$ represent the sum of the bond angles around the C or N atom, respectively

The remaining coordination position is occupied by a chlorido ligand. The structural features of the $CN_3$ moiety indicate charge delocalization among the four involved atoms. Thus, the three CN bonds lengths (see, for instance, N(2)−C(17): 1.310(4) Å,

N(3)−C(17): 1.361(4) Å and N(4)−C(17): 1.364(4) Å in complex **1**) exhibit intermediate values between CN single (1.47Å) and double bond (1.29 Å), with a shorter bond length involving the nitrogen atom coordinated to the metal. Moreover, accepting the experimental inaccuracy in the determination of bond angles involving hydrogen atoms, the geometry around the four atoms is almost planar (see Table 1).

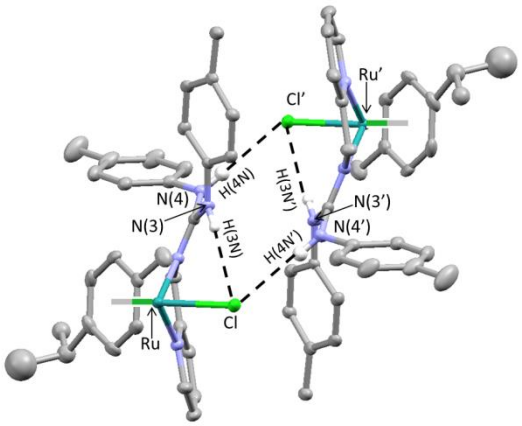


**Figure 2** Intra- and intermolecular interactions in complex **1**. For clarity all the hydrogen atoms are omitted, except the N-H protons. Primed atoms are related to non-primed ones through 2-*x*, 2-*y*, 1-*z* symmetry operation.

**Table 2.** Geometrical parameters (Å, °) of the H-bond interactions of complexes **1** and **2**.

| Complex | D-H···A | D-H | D···A | H···A | D-H···A |
|---|---|---|---|---|---|
| **1** | N(3)-H(3N)···Cl | 0.82(2) | 3.238(3) | 2.49(2) | 151(2) |
| **1** | N(4)-H(4N)···Cl' | 0.85(3) | 3.407(3) | 2.61(3) | 158(3) |
| **2** | N(2)-H(2N)···Cl(1) | 0.926(16) | 3.282(3) | 2.46(4) | 148(4) |
| **2** | N(3)-H(3N)···F(2'') | 0.906(16) | 2.989(3) | 2.11(4) | 163(4) |
| **2** | N(52)-H(52N)···Cl(51) | 0.912(16) | 3.318(3) | 2.61(5) | 134(4) |
| **2** | N(53)-H(3N)···F(11) | 0.921(17) | 2.896(3) | 2.02(5) | 159(4) |

Symmetry operations: ') 2-*x*, 2-*y*, 1-*z;* '') *x*, 1+*y*, *z*.

The NH protons of the guanidine fragments are involved in hydrogen bond interactions, whose geometrical parameters are compiled in Table 2. In complex **1**, the NH group *cis* to the ruthenium atom, H(3N), establishes an intramolecular hydrogen bond interaction with the chlorido ligand. However, the NH group *trans* to the metal, H(4N), interacts with the chlorido ligand of a neighbouring molecule, leading to the formation of inversion pairs of enantiomers through the $R(12)_4^4$ graph set depicted in Figure 2.[46] In complex **2**, a similar intramolecular NH···Cl interaction is observed involving NH group

*cis* to the ruthenium atom, whereas the NH group *trans* to the metal is interacting with fluorine atoms of the counterions.

**Reaction of the dimer [{($\eta^6$-*p*-cymene)RuCl}$_2$($\mu$-Cl)$_2$] with the phosphano-guanidine $H_2$L3**

Under the same conditions as for ligands **$H_2$L1** and **$H_2$L2**, the dimer [{($\eta^6$-*p*-cymene)RuCl}$_2$($\mu$-Cl)$_2$] reacts with the phospano-guanidine **$H_2$L3** giving rise to the new complexes [($\eta^6$-*p*-cymene)RuCl$_2$(**$H_3$L3**)][$SbF_6$] (**4**, 41 % yield) and [($\eta^6$-*p*-cymene)Ru($\kappa^3$*N*,*N'*,*P*-**HL3**)][$SbF_6$] (**10**, 34 % yield) together with the expected chlorido compound [($\eta^6$-*p*-cymene)RuCl(**$H_2$L3**)][$SbF_6$] (**3**, 14 % yield), (Scheme 5).[47] Formally, complexes **4** and **10** can be considered the products of the reaction of the ruthenium dimer [{($\eta^6$-*p*-cymene)RuCl}$_2$($\mu$-Cl)$_2$] with the guanidinium and guanidinate ions derived from the self-dissociation of neutral phosphano-guanidine **$H_2$L3** (Scheme 6).

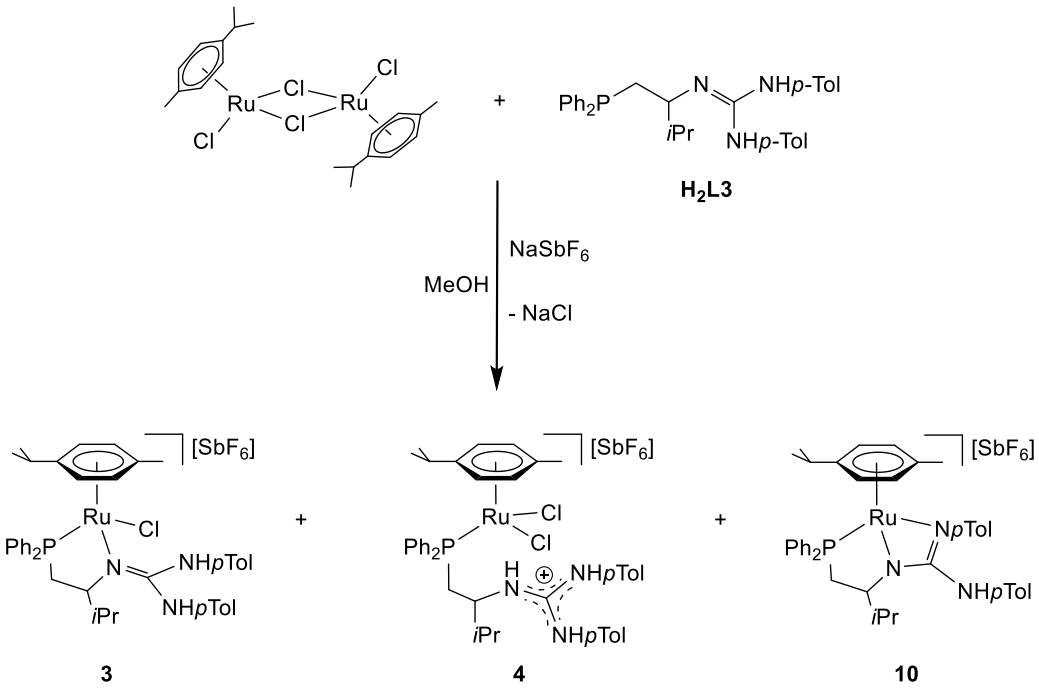


**Scheme 5.** Reaction of the dimer [{($\eta^6$-*p*-cymene)RuCl}$_2$($\mu$-Cl)$_2$] with **$H_2$L3**.

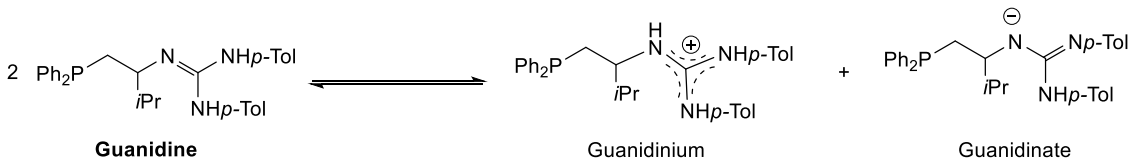


**Scheme 6**. Equilibrium of self-ionization of the phosphano-guanidine **$H_2$L3**.

In the reaction with the ruthenium dimer, the *S* at carbon enantiomer of the ligand **$H_2$L3** was employed. Complex **3** was obtained as an equimolar mixture of the $R_{Ru}$,$S_C$ and $S_{Ru}$,$S_C$ diastereomers. Complex **10** was present as an 87/13, $R_{Ru}$,$S_N$,$S_C$/$S_{Ru}$,$R_N$,$S_C$ molar mixture of diastereomers that epimerizes to a molar ratio $R_{Ru}$,$S_N$,$S_C$/$S_{Ru}$,$R_N$,$S_C$ of 98/2, when the mixture was heated at 323 K in methanol for 3 days. Complex **10** was prepared by an alternative route as we will discuss below. A mixture of complex **4** (96 %) and complex **3** (4 %) was obtained by treating complex **10** with aqueous HCl. The $^1$H NMR spectrum of compound **4** reveals the presence of three inequivalent NH protons at 9.24, 6.76 and 5.38 ppm, the latter assigned to the NH bonded to the CH(*i*Pr) moiety, confirming the protonation of the guanidine ligand.

**Synthesis of the aqua complexes [($\eta^6$-*p*-cymene)Ru($H_2$L)($OH_2$)][$SbF_6$]$_2$ ($H_2$L = $H_2$L1 (5), $H_2$L2 (6), $H_2$L3 (7))**

The dicationic aqua-complexes [($\eta^6$-*p*-cymene)Ru(**$H_2$L**)($OH_2$)][$SbF_6$]$_2$ (**$H_2$L** = **$H_2$L1**, (**5**), **$H_2$L2** (**6**)) were obtained by treating the corresponding chlorido complexes **1** and **2** with $AgSbF_6$, in acetone, at room temperature. Treatment a mixtures of the complexes **3**, **4** and **10** with $AgSbF_6$ afforded the analogue aqua-complex with the **$H_2$L3** ligand, [($\eta^6$-*p*-cymene)Ru(**$H_2$L3**)($OH_2$)][$SbF_6$]$_2$ (**7**), in overall yield of 92 % (Scheme 7). The presence of trace amounts of water in the solvent is sufficient for these aqua-complexes to form. All of these complexes were stable at room temperature and characterised *via* IR and NMR spectroscopy, elemental analysis (see Experimental Section) and by the determination of the X-ray crystal structure of complex **5**.

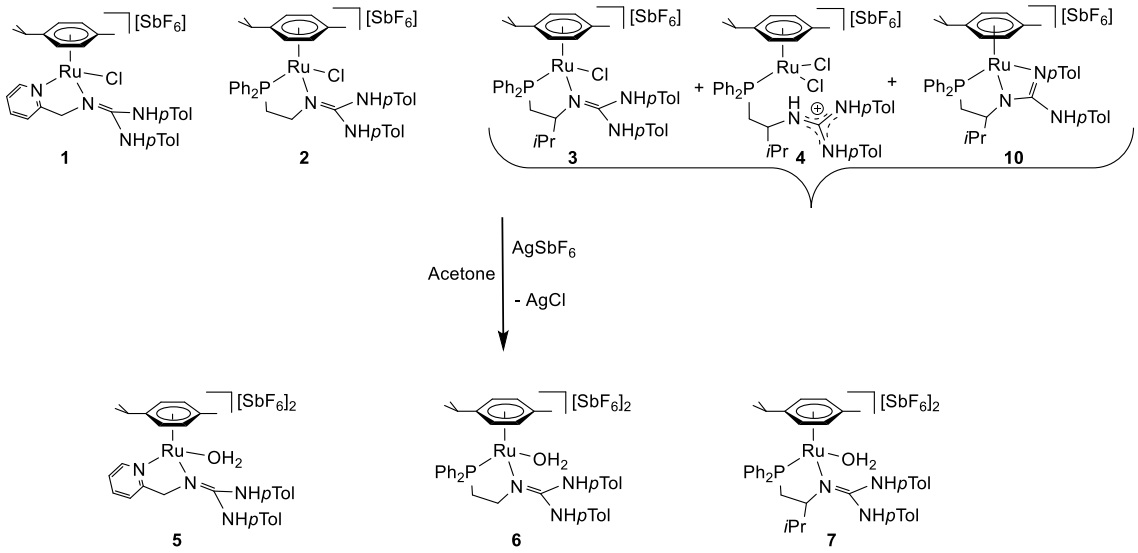


**Scheme 7**. Preparation of the aqua complexes **5**-**7**.

The $^{1}$H NMR spectra of these complexes clearly establish that the *p*-cymene/**H$_2$L** molar ratio is 1/1. The diastereomeric nature of the methylene protons indicates that the guanidine ligand adopts a chelate $\kappa^2$*N,N'* or $\kappa^2$*N,P* coordination mode that renders the metal a stereogenic centre. NOE interactions between the methylene and the *p*-cymene protons allows to distinguish between *pro-R* and *pro-S* methylene protons. The formation of complex **7** is diastereoselective being obtained as a mixture of diastereomers in *ca.* 63/37 molar ratio. Whereas in the most abundant isomer were observed NOE interactions between the CH proton of the isopropyl group of the guanidine ligand and the methyl group of the *p*-cymene ligand, in the minor isomer the NOESY spectrum showed interaction between the proton bound to the stereogenic carbon and the protons of the methyl groups of the isopropyl substituent of the *p*-cymene ligand. These data allow to assign the $R_{Ru}$,$S_C$ configuration to the major isomer and the $S_{Ru}$,$S_C$ configuration to the less abundant isomer (Scheme 8).

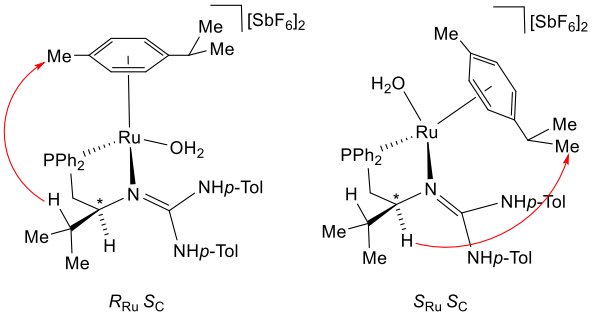


**Scheme 8**. Selected NOE interactions in the diastereomers of complex **7**.

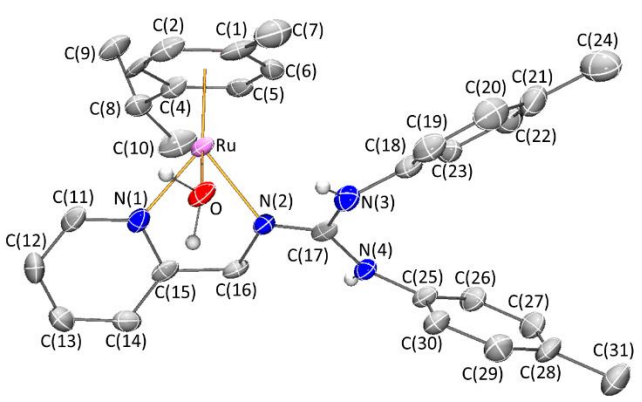


**Figure 3**. Molecular structure of the cation of complex **5**. For clarity all the hydrogen atoms are omitted, except the NH protons.

**Table 3**. Selected bond lengths (Å) and angles (º) for complex **5**.

| | | | |
|---|---|---|---|
| Ru-O | 2.184(8) | N(2)-Ru-Ct[a] | 135.45(1) |
| Ru-N(1) | 2.083(10) | N(2)-C(16) | 1.476(14) |
| Ru-N(2) | 2.090(9) | N(2)-C(17) | 1.307(15) |
| Ru-Ct[a] | 1.6834(1) | N(3)-C(17) | 1.364(16) |
| O-Ru-N(1) | 83.8(3) | N(4)-C(17) | 1.374(13) |
| O-Ru-N(2) | 80.5(3) | $\sum \widehat{C(17)}$[b] | 360.0(2) |
| O-Ru-Ct[a] | 130.82(1) | $\sum \widehat{N(2)}$[b] | 359.6(13) |
| N(1)-Ru-N(2) | 77.4(4) | $\sum \widehat{N(3)}$[b] | 358(14) |
| N(1)-Ru-Ct[a] | 131.75(1) | $\sum \widehat{N(4)}$[b] | 357(11) |

[a] Ct stands for the centroid of the *p*-cymene ligand. [b] $\sum \hat{C}$ and $\sum \hat{N}$ represent the sum of the bond angles around the C or N atom, respectively.

The crystal structure of complex **5** was determined by X-ray diffraction methods. Complex **5** crystallises in the $P\bar{1}$ centrosymmetric space group and, therefore, the two enantiomers are present in the unit cell. A view of the $S_{Ru}$ cation is depicted in Figure 3 and relevant bond lengths and angles are collected in Table 3. An $\eta^6$-*p*-cymene group occupies three *fac* coordination positions and the ligand **H$_2$L1** adopts a chelate $\kappa^2 N,N'$

coordination mode. A water molecule completes the pseudooctahedral coordination of the metal.

The structural parameters of the $CN_3$ guanidine group resembles to those determined for complexes **1** and **2**, with a shortening of CN bond distance involving coordinated nitrogen (N(2)-C(17): 1.307(15) Å) compared to the two remaining CN bonds (N(3)-C(17): 1.364(13) Å, N(4)-C(17): 1.374(13) Å). As for complexes **1** and **2**, a planar geometry around the four $CN_3$ atoms was also observed (see Table 3).

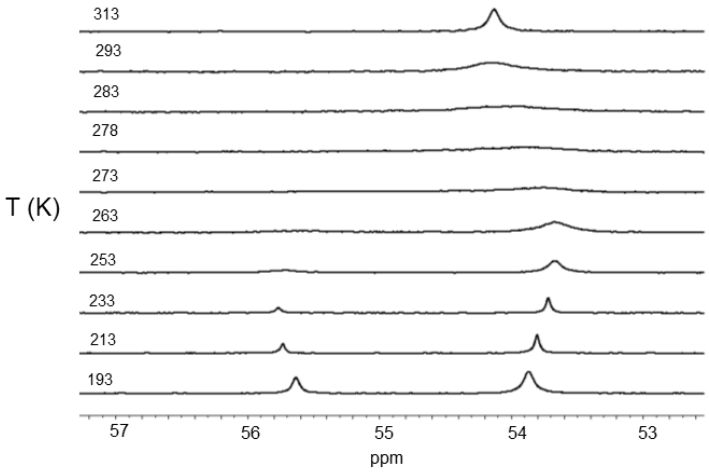


**Figure 4**. Variation with temperature of the $^{31}P\{^{1}H\}$ NMR spectra of complex **6** in $CD_2Cl_2$.

From 313 to 193 K, no significant changes have been found in the NMR spectra of the chlorido complexes **1-3**. However, several $^{1}H$ and $^{31}P$ NMR signals of the aqua complexes **5-7** broaden and split as temperature decreases. In particular, at 193 K, the $^{31}P\{^{1}H\}$ NMR spectrum of complex **6** showed two broad singlets centred at about 55.6 and 53.9 ppm, in about 1/2 molar ratio, respectively, which coalesce to one unique singlet at 54.1 ppm, by heating the sample up to 313 K. These spectroscopic data suggest that the complex undergoes a fluxional process. From the equilibration of the phosphorus nuclei, the free energy of activation, $\Delta G^{\#}$, at the coalescence temperature (276 K), for the process has been calculated: $\Delta G^{\#} = 13.17 \pm 0.12$ kcal·mol$^{-1}$.[48,49]

DFT calculations have been carried out to obtain information about the NMR behaviour observed in solution. The NMR experimental data can be accounted for by assuming the interconversion between two rotamers **6a** and **6b** (Figure 5). These rotamers are characterised by the values of the dihedral angle N−C−N−C(aryl) involving the NC−(NH*p*Tol)$_2$ core of the guanidino ligand (146.5º, **6a**; -22.3º, **6b**). The calculated activation barrier of 12.1 kcal·mol$^{-1}$ is in good agreement with the $\Delta G^{\#}$ determined from experimental NMR data. The calculated Gibbs free energy difference between the two rotamers is 0.6 kcal·mol$^{-1}$; this low value, probably below the precision of the calculation method, is compatible with the equilibrium experimentally detected between the two rotamers. The fluxional behaviour of complex **6** (probably similar to that of complexes **5** and **7**) parallels that found in the related osmium complexes, we have recently reported.[42]

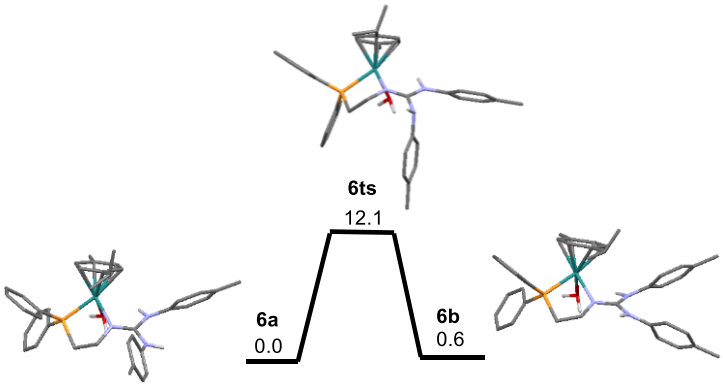


**Figura 5**. Gibbs free energy profile of the equilibrium between rotamers **6a** and **6b**. Free energies are in kcal·mol$^{-1}$.

**Synthesis of the complexes [($\eta^6$-*p*-cymene)Ru(HL)][SbF$_6$] (H$_2$L = H$_2$L1 (8), H$_2$L2 (9), H$_2$L3 (10))**

At room temperature, complexes **5**, **6** and **7** reacted with stoichiometric amounts of NaHCO$_3$, in methanol affording the deprotonated complexes **8**, **9** and **10**, respectively, in 93-95 % yield (Scheme 10). Addition of aqueous HSbF$_6$ to complexes **9** and **10** regenerates the corresponding starting compounds.

The new complexes were stable at room temperature and characterised using both IR and NMR spectroscopy, elemental analysis and X-Ray crystallography for complexes **9** and **10**. In complexes **8** and **9**, the metal and the $CH_2N$ nitrogen of the guanidine ligand are stereogenic centres. The formation of these complexes is completely diastereoselective since only one enantiomeric pair of diastereomers is detected and according to the NOE relationship between the $H_{pro\text{-}S}$ nucleus of the methylene adjacent to the stereogenic nitrogen and *p*-cymene protons their absolute configuration is $S_{Ru},R_N/R_{Ru},S_N$ in both cases. Because the methylene carbon adjacent to the stereogenic nitrogen is also a stereogenic centre, complex **10** was obtained as a mixture of two diastereomers in an 83/17 molar ratio. From NOE data similar to those mentioned for complexes **8** and **9**, the configuration of the obtained diastereomers is $S_{Ru},R_N,S_C$ and $R_{Ru},S_N,S_C$, the latter configuration corresponding to the most abundant isomer. Pure samples of $R_{Ru},S_N,S_C$-**10** were obtained by recrystallization from methanol. Slow epimerisation at ruthenium was observed. Thus, when a 71/29 $R_{Ru},S_N,S_C/S_{Ru},R_N,S_C$-**10** molar ratio mixture was heated, during 5 days, at 323 K, in dichloromethane, a mixture containing 98 % of $R_{Ru},S_N,S_C$-**10** and 2 % of $S_{Ru},R_N,S_C$-**10** was recovered.

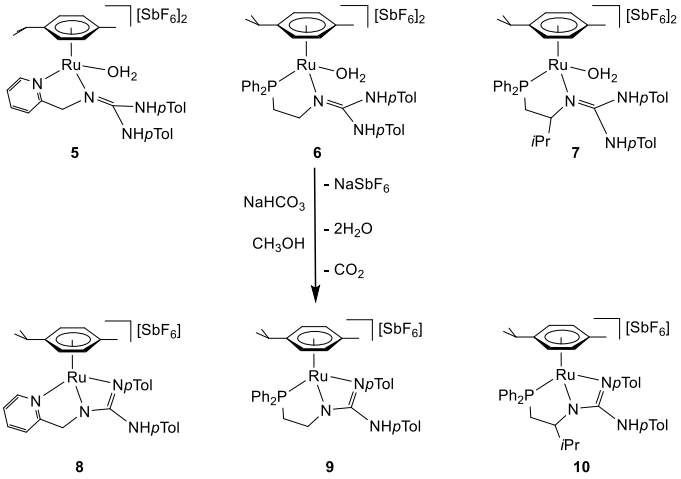


**Scheme 10.** Preparation of the complexes **8**-**10**.

A weak IR band around 3370 $cm^{-1}$and a singlet in the $^{1}H$ NMR spectrum at *ca*. 5.8 ppm are attributed to the only remaining NH functionality. A singlet at 55.93 ppm (complex **9**) and at 49.65 ppm (major) and 48.98 (minor) (complex **10**) in the $^{31}P\{^{1}H\}$ NMR spectrum revealed the presence of a coordinated $PPh_2$ group in these complexes.

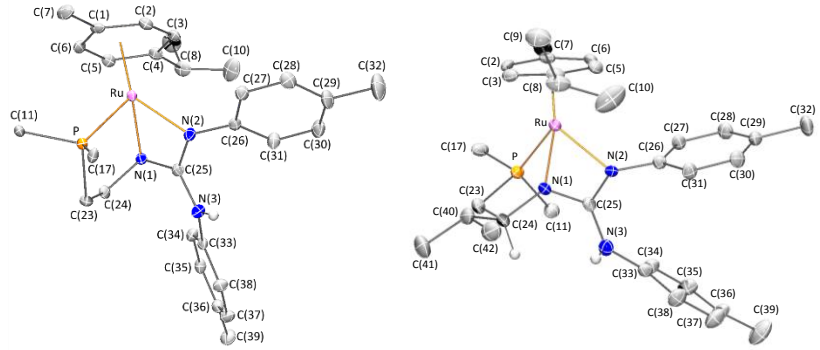


**Figure 6.** Molecular structure of the cations of complexes **9** and **10**. For clarity, all the hydrogen atoms are omitted, except the NH protons and the hydrogen atom of the stereogenic carbon atom of complex **10**. For complex **10**, only the *ipso* carbon atoms of phenyl groups of the phosphine fragment have been depicted.

**Table 4**. Selected bond lengths (Å) and angles (º) for complexes **9** and **10**.

| | **9** | **10** |
|---|---|---|
| Ru-P | 2.3384(15) | 2.3109(13) |
| Ru-N(1) | 2.120(5) | 2.122(4) |
| Ru-N(2) | 2.091(5) | 2.098(4) |
| Ru-Ct[a] | 1.7047(1) | 1.7120(1) |
| P-Ru-N(1) | 78.61(14) | 75.09(13) |
| P-Ru-N(2) | 91.53(15) | 91.33(12) |
| P-Ru-Ct[a] | 133.17(1) | 133.48(1) |
| N(1)-Ru-N(2) | 62.5(2) | 62.38(16) |
| N(1)-Ru-Ct[a] | 133.91(1) | 135.96(1) |
| N(2)-Ru-Ct[a] | 130.79(1) | 131.22(1) |
| Ru-N(1)-C(25) | 92.8(4) | 93.4(3) |
| Ru-N(2)-C(25) | 95.0(4) | 95.4(3) |
| N(1)-C(25)-N(2) | 109.2(5) | 108.8(4) |
| N(1)-C(24) | 1.472(8) | 1.476(6) |
| N(1)-C(25) | 1.356(8) | 1.360(6) |
| N(2)-C(25) | 1.325(8) | 1.327(6) |
| N(3)-C(25) | 1.361(8) | 1.368(6) |
| $\sum \widehat{C(25)}$[b] | 359.7(10) | 360.7(7) |
| $\sum \widehat{N(1)}$[b] | 329.5(7) | 340.8(6) |
| $\sum \widehat{N(2)}$[b] | 355.2(7) | 351.1(6) |
| $\sum \widehat{N(3)}$[b] | 358(7) | 359(6) |

[a] Ct stands for the centroid of the *p*-cymene ligand. [b] $\sum \hat{C}$ and $\sum \hat{N}$ represent the sum of the bond angles around the C or N atom, respectively.

The molecular structure of complexes **9** and **10** has been determined by X-ray diffraction means. Complex **9** crystallises as racemate in the $Pna2_1$ group of the orthorhombic system. Complex **10** crystallises in the chiral $P2_12_12_1$ space group, and therefore only one diastereomer is present in the unit cell. Views of the cation of the $S_{Ru}$,$R_N$ enantiomer of complex **9** and that of the $R_{Ru}$,$N_N$,$S_C$ diastereomer of compound **10** are depicted in Figure 6. Relevant bond lengths and angles for both complexes are collected in Table 4.

In the context of the present work, some of the structural features encountered in complexes **9** and **10** deserve to be commented:

i) The **HL2** ligand in complex **9** and the **HL3** ligand in complex **10** both present *fac* $\kappa^3$*N,N',P* coordination mode.

ii) In both complexes, the N(1) atom of the guanidine ligand adopts a pyramidal $sp^3$ geometry: $\Sigma^o$N(1) = 329.5(7)º in **9** and 340.8(6)º in **10**.

iii) This geometry contrasts with the $sp^2$ hybridisation that this nitrogen atom presents when the **$H_2$L** ligands coordinate in a chelate $\kappa^2$*N,P* manner (compounds **1**, **2** and **5**).

iv) In both complexes, the N(2) coordinated nitrogen atom of the guanidine ligand presents an essentially planar geometry: $\Sigma^o$N(2) = 355.7(4)º in **9** and 351.1(6)º in **10**. Also the $CN_3$ core of the guanidine ligand is essentially planar in both complexes as well as, in the cation of the complexes **1**, **2** and **5**. The structural parameters encountered are compatible with a charge delocalisation among the four involved atoms that, most probably, contributes to the stabilisation of the cation of the compounds.

v) The small values of the N(1)-Ru-N(2) (complex **9**: 62.36(11)º, complex **10**: 62.37(16)º) and N(1)-C(25)-N(2) (complex **9**: 108.8(4)º, complex **10**: 109.7(4)º) bond angles, far from the ideal hybridisation values, reflect the strain of the four-membered Ru-N(1)-C(25)-N(2) metallacycle for both complexes.

All these structural characteristics indicate that complexes **9** and **10** (and, most probably also complex **8**) fulfil the necessary requirements to anticipate potential FLP reactivity for them.

## Conclusions

In summary, half-sandwich ruthenium(II) complexes of formula [($\eta^6$-*p*-cymene)Ru(**HL**)][$SbF_6$] in which pyridinyl- or phosphano-guanidinate ligands present *fac* $\kappa^3$*N,N',N''* or $\kappa^3$*N,N',P* coordination modes can be efficiently prepared starting from the dimer [{($\eta^6$-*p*-cymene)RuCl}$_2$($\mu$-Cl)$_2$] *via* the corresponding chlorido [($\eta^6$-*p*-cymene)RuCl(**H$_2$L**)][$SbF_6$] and aqua [($\eta^6$-*p*-cymene)Ru(**H$_2$L**)($OH_2$)][$SbF_6$]$_2$ complexes. As key structural motive, the central nitrogen atom of the guanidine ligand changes its hybridisation from $sp^2$ to $sp^3$ on going from chelate $\kappa^2$ coordination mode in the aqua complexes **5**-**7** to *fac* $\kappa^3$coordination mode in complexes **8**-**10**. As a consequence of the coordination mode, the latter exhibit a strained four-membered Ru−N−C−N metallacycle. It can be anticipated that this metallacycle would be easily opened giving place to FLP species in which the metal and a nitrogen atom can play the role of Lewis acid and Lewis base components, respectively. Future work in our group will aim to apply these type of compounds in activation of small molecules as well as in catalytic reactions.

## Experimental Section

*General information*

All preparations have been carried out under argon. All solvents were treated in a PS-400-6 Innovative Technologies Solvent Purification System (SPS) and degassed prior to use. Infrared spectra were recorded on Perkin-Elmer Spectrum-100 (ATR mode) FT-IR spectrometer. Carbon, hydrogen and nitrogen analyses were performed using a Perkin-Elmer 240 B microanalyser. $^{1}$H, $^{13}$C and $^{31}$P NMR spectra were recorded on a Bruker AV-300 spectrometer (300.13 MHz), Bruker AV-400 (400.16 MHz) or Bruker AV-500 (500.13 MHz). In both $^{1}$H NMR and $^{13}$C NMR measurements the chemical shifts are expressed in ppm downfield from $SiMe_4$. The $^{31}$P NMR chemical shifts are relative to 85 % $H_3PO_4$. *J* values are given in Hz. NOESY and $^{13}$C, $^{31}$P and $^{1}$H correlation spectra were obtained using standard procedures. Mass spectra were obtained with a Micro Tof-Q Bruker Daltonics spectrometer.

*Preparation of the phosphino-guanidino ligand* ***$H_2$L3***

(*S*)-1-(diphenylphosphino)-2-amino-3-methylbutane (142.9 $\mu$L, 0.55 mmol) was dissolved in dry THF (10 mL) and, to the resulting solution, 1,3-di-*p*-toylcarbodiimide (122.9 mg, 0.55 mmol) was added. Under argon atmosphere, the reaction was stirred for *ca*. 15 h, at room temperature. THF was removed by vacuum evaporation. The resulting oil was washed with *n*-hexane (3 × 10 mL) and vacuum-dried. The resulting dense oil was used in the reactions with the ruthenium precursor without further purification.

*$^{1}$H NMR (500.10 MHz, $CD_2Cl_2$, RT):* $\delta$ = 7.53-7.29 (m, 10H, $PPh_2$), 7.08 (d, *J* = 8.1 Hz, 4H, CH *p*-Tol), 6.87 (bs, 4H, CH *p*-Tol), 5.54 (bs, 1H, NH), 4.00 (bs, 2H, NH, C*-H),

2.40, 2.24 (2 × m, 2H, $PCH_2$), 2.30 (s, 6H, Me *p*-Tol), 2.04 (m, 1H, CH *i*Pr), 0.92, 0.86 (2 × d, *J* = 6.8 Hz, 6H, Me *i*Pr).

*$^{13}C\{^1H\}$ NMR (125.77 MHz, $CD_2Cl_2$, RT):* $\delta$ = 148.43 (C=N), 141.63 (d, *J* = 8.9 Hz), 140.22 (d, *J* = 12.9 Hz), 133.91-133.39, 129.48-129.15 ($PPh_2$), 130.61 (Ar *p*-Tol), 54.02 C*-H, 33.46 (CH *i*Pr), 32.66 (d, *J* = 14.0 Hz, $CH_2P$), 21.29 (Me *p*-Tol), 19.61, 18.47 (Me *i*Pr).

*$^{31}P\{^1H\}$ NMR (202.46 MHz, $CD_2Cl_2$, RT):* $\delta$ = -23.02 (s).

*Preparation of the complexes [($\eta^6$-p-cymene)RuCl(**$H_2$L**)][$SbF_6$] (**$H_2$L = $H_2$L1 (1) $H_2$L2 (2)***

The dimer [{($\eta^6$-*p*-cymene)RuCl}$_2$($\mu$-Cl)$_2$] (800.0 mg, 1.31 mmol) and $NaSbF_6$ (675.8 mg, 2.62 mmol) were added to a solution of corresponding the **$H_2$L** ligand (2.62 mmol) in MeOH (10 mL). The orange/yellow solution was stirred under argon for 5 h, at room temperature. The resulting suspension was vacuum-evaporated until dryness and the residue was extracted with $CH_2Cl_2$ (20 mL). The solution was vacuum-evaporated until *ca.* 2 mL and *n*-pentane (20 mL) was added, resulting in the precipitation of a yellow (complex **1**) or orange (complex **2**) solid. The suspension was decanted to remove pentane and the solid was washed with *n*-pentane (2 × 10 mL) and vacuum-dried. The product was recrystallised from methanol/$Et_2O$. Single crystals of the complex were developed by slow diffusion of MeOH into a $Et_2O$ solution.

Complex **1**. Yield: 1497.1 mg, 70 %. Anal. Calcd for $C_{31}H_{36}N_4ClF_6RuSb$: C, 44.5; H, 4.3; N, 6.7. Found: C, 44.9; H, 4.6; N, 6.9. HRMS ($\mu$-TOF), $C_{31}H_{36}N_4ClF_6RuSb$, $[M-SbF_6]^+$, calcd: 601.1671, found: 601.1661. IR ($cm^{-1}$): $\nu$(NH) 3291 (br); $\nu$(N=C) 1624 (m), 1608 (m); $\nu(SbF_6)$ 653 (s).

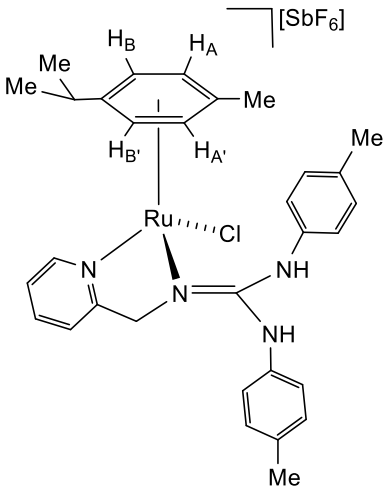


*S*Ru-**1**

*S*Ru-**1** enantiomer. *$^{1}$H NMR (500.10 MHz, $CD_2Cl_2$, RT):* $\delta$ = 8.93 (d, *J* = 5.5 Hz, 1H, $H_6$Py), 8.58 (s, 1H, NH *trans* $CH_2$), 7.86 (t, *J* = 8.8 Hz, 1H, $H_4$Py), 7.46 (t, *J* = 7.8 Hz, 1H, $H_5$Py), 7.40 (s, 1H, NH *trans* Ru), 7.32 (d, *J* = 7.9 Hz, 1H, $H_3$Py), 7.03 (d, *J* = 8.0 Hz), 6.99 (d, *J* = 8.2 Hz), 6.94 (bd) (8H, CH *p*-Tol), 5.68 (d, *J* = 5.8 Hz, 1H, $H_B$), 5.62 (d, *J* = 6.1 Hz, 1H, $H_{A'}$), 5.50 (d, 1H, $H_{B'}$), 5.44 (d, 1H, $H_A$), 5.03 (d, *J* = 17.9 Hz, 1H, $H_{pro\text{-}R}$ $CH_2$), 4.98 (d, 1H, $H_{pro\text{-}S}$ $CH_2$), 2.58 (spt, 1H, CH *i*Pr *p*-cymene), 2.23, 2.21 (2 × s, 6H, Me *p*-Tol), 2.06 (s, 3H, Me *p*-cymene), 1.12 and 1.10 (2 × d, *J* = 7.0 Hz, 6H, 2 × Me *i*Pr *p*-cymene).

*$^{13}C\{^{1}H\}$ NMR (125.77 MHz, $CD_2Cl_2$, RT)*: $\delta$ = 162.30 ($C_2$Py), 154.97 (C=N), 154.92 ($C_6$Py), 139.97 ($C_4$Py), 136.49, 136.43, 134.50, 134.22, 130.92, 130.46, 120.64, 119.95 (Ar *p*-Tol), 125.86 ($C_5$Py), 121.79 ($C_3$Py), 107.13 (C−*i*Pr *p*-cymene), 98.97 (C−Me *p*-cymene), 88.26 ($CH_{A'}$), 85.28 ($CH_A$), 84.09 ($CH_{B'}$), 81.78 ($CH_B$), 61.08 ($CH_2$), 31.98 (CH *i*Pr), 23.24, 21.82 (2 × Me *i*Pr *p*-cymene), 21.20 (2 × Me *p*-Tol) and 18.98 (Me *p*-cymene).

Complex **2**. Yield: 2758.5 mg, 81 %. Anal. Calcd for $C_{39}H_{44}N_3ClF_6RuPSb$: C, 48.9; H, 4.6; N, 4.4. Found: C, 48.5; H, 4.7; N, 4.2. HRMS ($\mu$-TOF), $C_{39}H_{44}N_3ClF_6RuPSb$, $[M\text{-}SbF_6]^+$, calcd: 722.2006, found: 722.2004. IR ($cm^{-1}$): $\nu$(NH) 3250-3445 (br), $\nu$(N=C) 1608 (m), $\nu(SbF_6)$ 654 (s).

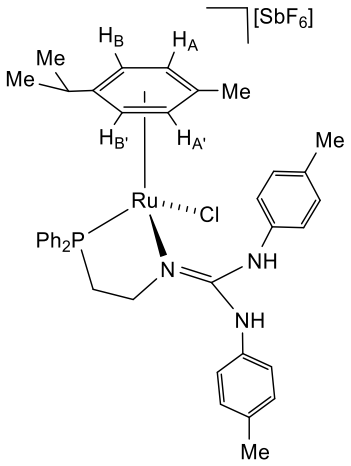


$S_{Ru}$-**2**

$S_{Ru}$-**2** enantiomer. *$^{1}$H NMR (500.10 MHz, $CD_2Cl_2$, RT):* $\delta$ = 9.00 (s, 1H, NH *trans* $CH_2$), 7.67 - 7.45 (m, 10H, $PPh_2$), 7.29 (s, 1H, NH *trans* Ru), 7.07, 6.94 (2 × d, *J* = 7.0 Hz, 4H CH *p*-Tol), 7.00, 6.93 (2 × d, *J* = 6.95 Hz, 4H CH *p*-Tol), 5.70 (d, *J* = 6.0 Hz, 1H, $H_A$), 5.56 (d, *J* = 6.1 Hz, 1H, $H_{B'}$), 5.13 (d, 1H, $H_B$), 5.04 (d, 1H, $H_{A'}$), 4.25 (dm, *J* = 44.4 Hz, 1H, $H_{pro\text{-}R}$ $NCH_2$), 3.45 (m, 1H, $H_{pro\text{-}S}$ $NCH_2$), 2.91 (m, 1H, $H_{pro\text{-}R}$ $PCH_2$)), 2.43 (spt, 1H, CH *i*Pr *p*-cymene), 2.25, 2.22 (2 × s, 6H, Me *p*-Tol), 2.16 (m, 1H, $H_{pro\text{-}S}$ $PCH_2$), 1.99 (s, 3H, Me *p*-cymene), 1.22 and 1.07 (2 × d, *J* = 6.8 Hz, 6H, 2 × Me *i*Pr *p*-cymene).

*$^{13}$C{$^{1}$H} NMR (125.77 MHz, $CD_2Cl_2$, RT):* $\delta$ = 155.85 (C=N), 136.8 (d, *J* = 47.2), 130.11 (d, *J* = 55.8 Hz), 134.20 - 129.47 $PPh_2$), 131.13, 130.50, 120.34, 119.01 Ar), 111.21 (*C*–$^{i}$Pr *p*-cymene), 100.31 (*C*–Me *p*-cymene), 93.65 ($CH_{A'}$), 90.33 ($CH_B$), 89.42 ($CH_A$), 85.51 ($CH_{B'}$), 55.08 ($CH_2N$), 31.62 ($CH_2P$), 31.42 (CH *i*Pr *p*-cymene), 22.84, 22.72 (2 × Me *i*Pr *p*-cymene), 21.19 (2 × Me *p*-Tol) and 18.44 (Me *p*-cymene).

*$^{31}$P{$^{1}$H} NMR (202.46 MHz, $CD_2Cl_2$, 193 K)*: $\delta$ = 56.86 (s).

*Reaction of the dimer [{($\eta^6$-p-cymene)RuCl}$_2$($\mu$-Cl)$_2$] with* ***H$_2$L3***

The dimer [{($\eta^6$-*p*-cymene)RuCl}$_2$($\mu$-Cl)$_2$] (206.0 mg, 0.34 mmol) and $NaSbF_6$ (174.2 mg, 0.68 mmol) were added to the **H$_2$L3** ligand (324.2 mg, 0.68 mmol), followed by the addition of methanol (10 mL). The resulting orange solution was stirred under argon for 2 h. The solution was vacuum-evaporated until dryness and the residue extracted with dichloromethane (20 mL). The resulting solution was vacuum-evaporated until *ca*. 2 mL and the slow addition of *n*-pentane (20 mL) led to the precipitation of an orange solid. The solid was washed with *n*-pentane (2 × 10 mL) and vacuum-dried. A mixture of [($\eta^6$-*p*-cymene)RuCl(**H$_2$L3**)][$SbF_6$] (**3**, 14%), [($\eta^6$-p-cymene)RuCl$_2$(**H$_3$L3**)][$SbF_6$] (**4**, 41%) and [($\eta^6$-*p*-cymene)Ru($\kappa^3$*N,N',P*-**HL3**)][$SbF_6$] (**10**, 34%) was obtained.

Complex **3**. HRMS ($\mu$-TOF), for $C_{42}H_{50}N_3ClF_6PRuSb$, $[M\text{-}SbF_6]^+$, calcd: 764.2477, found: 764.2511.

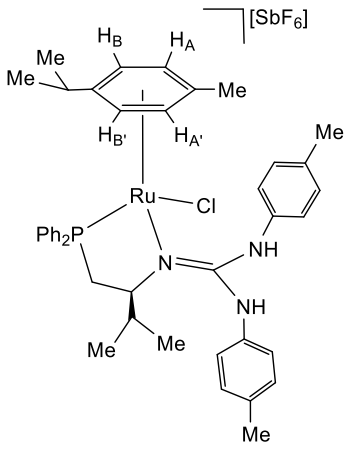


**3**

*$^1$H NMR (500.10 MHz, $CD_2Cl_2$, RT):* $\delta$= 1.73 (s, 3H, Me *p*-cymene), 1.13, 1.01 (d, $J$ = 6.9 Hz), 0.91, 0.87 (2 × d, $J$ = 6.7 Hz, 6H, 2 × Me *i*Pr *p*-cymene and 2 × Me *i*Pr **H$_2$L3** ligand).

*$^{31}$P{$^1$H} NMR (202.46 MHz, $CD_2Cl_2$, RT):* $\delta$ = 54.63 (s) (major), 57.39 (s) (minor).

*Preparation of the complex [($\eta^6$-p-cymene)$RuCl_2$(**$H_3$L3**)][$SbF_6$] (**4**) from complex **10***

To a solution of the complex [($\eta^6$-*p*-cymene)Ru($\kappa^3$*P,N,N'*-**HL3**)][$SbF_6$] (**10**) (40 mg, 0.041 mmol) in dichloromethane (2 mL) was added 17 µL (0.205 mmol) of aqueous HCl (37 %, w/w; $\rho$ = 1.19 g·$mL^{-1}$). The resulting solution was stirred for 15 min and concentrated under reduced pressure to *ca.* 0.5 mL. The slow addition of *n*-pentane led to the precipitation of an orange solid which was washed with water (2 × 0.5 mL) and pentane (3 × 1 mL) and vacuum-dried. According to NMR measurements, the solid consist of a 96/4, **4**/**3** mixture.

Complex **4**. HRMS ($\mu$-TOF), $C_{42}H_{51}N_3Cl_2F_6RuPSb$, $[M\text{-}SbF_6]^+$, calcd: 800.2241, found: 800.2267. IR ($cm^{-1}$): ν(NH) 3339-3055 (br), ν(N=C) 1629 (br), 1599 (m), ν($SbF_6$) 656 (s).

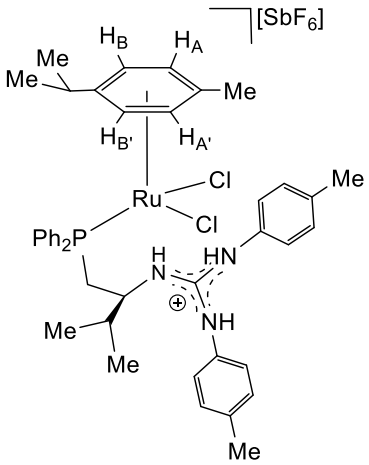


**4**

*$^1$H NMR (500.10 MHz, $CD_2Cl_2$, RT):* $^1$H NMR (500.10 MHz, $CD_2Cl_2$, RT): $\delta$ = 9.24 (bs, 1H, NH), 7.90 - 7.50 (m, 10H, $PPh_2$), 7.22 - 6.94 (m, 8H, CH *p*-Tol), 6.76 (bs, 1H, NH), 5.38 (bs, 1H, NHC*), 5.26 (d, *J* = 6.2 Hz, 2H, $H_B$), 5.18 (d, 1H, $H_A$), 5.07 (d, *J* = 6.0 Hz, 2H, $H_{A'}$), 4.99 (d, 1H, $H_{B'}$), 4.61 (m, 1H, C*H), 2.96, 2.60 (2 × m, 2H, $PCH_2$), 2.63 (spt, 1H, CH *i*Pr *p*-cymene), 2.30 (bs, 6H, Me *p*-Tol), 1.92 (s, 3H, Me *p*-cymene), 1.52 (spt,

1H, CH *i*Pr **H$_3$L3**), 1.12, 1.11 (2 × d, *J* = 6.9 Hz, 6H, 2 × Me *i*Pr *p*-cymene), 0.80, 0.57 (2 × d, *J* = 6.7 Hz, 6H, 2 × Me *i*Pr **H$_3$L3**).

*$^{13}C\{^1H\}$ NMR (125.77 MHz, $CD_2Cl_2$, RT):* $\delta$ = 153.47 (C=N), 134.88 - 129.51 ($PPh_2$), 131.32, 130.97 (Ar *p*-Tol), 111.28 (*C*−*i*Pr *p*-cymene), 97.77 (*C*−Me *p*-cymene), 90.43 ($CH_A$), 90.00 ($CH_{A'}$), 88.53 ($CH_B$), 86.92 ($CH_{B'}$), 55.28 (C*), 33.90 (d, *J* = 6.6 Hz, CH *i*Pr **H$_3$L3**), 32.41 (d, *J* = 25.8 Hz, $CH_2P$), 31.17 (CH *i*Pr *p*-cymene), 22.55, 22.37 (2 × Me *i*Pr *p*-cymene), 21.51 (2 × Me *p*-Tol), 20.17, 15.12 (2 × Me *i*Pr **H$_3$L3**), 18.51 (Me *p*-cymene).

*$^{31}P\{^1H\}$ NMR (202.46 MHz, $CD_2Cl_2$, RT):* $\delta$ = 19.35 (s).

*Preparation of the complexes [($\eta^6$-p-cymene)Ru(**H$_2$L**)($OH_2$)][$SbF_6$]$_2$ (**H$_2$L** = **H$_2$L1 (5)**, **H$_2$L2 (6)**, **H$_2$L3 (7)**)*

To solutions of the complexes **1** or **2** (0.60 mmol) in acetone (15 mL), $AgSbF_6$ (205.3 mg, 0.60 mmol) was added. Precipitation was observed immediately and the mixture stirred for *ca*. 4 h whilst covered from light. The resulting suspension was filtered and the filtrate vacuum-evaporated until *ca.*1 mL. The addition of *n*-pentane (10 mL) led to the precipitation of an orange/yellow (**5**) or orange (**6**) solid. The resulting solid was washed with *n*-pentane (2 × 10 mL) and vacuum-evaporated until dryness. Single crystals were obtained by slow diffusion of *n*-pentane into dichloromethane solutions of complex **5**.

Starting from a mixture of complexes **3**, **4** and **10**, complex **7** was similarly prepared. It was isolated as a 63/37, $R_{Ru}$,$S_C$/$S_{Ru}$,$S_C$ mixture of diastereomers.

Complex **5**. Yield: 494.8 mg, 79 %. Anal. Calcd for $C_{31}H_{38}N_4F_{12}ORuSb_2$: C, 35.3; H, 3.6; N, 5.3. Found: C, 35.4; H, 3.5; N, 5.5. HRMS ($\mu$-TOF), $C_{31}H_{38}N_4F_{12}ORuSb_2$, [M-2$SbF_6$-

$H_2O$-H]$^+$, calcd: 565.1908, found: 565.1919. IR (cm$^{-1}$): *v*(NH), *v*(OH) 3386 (br), *v*(N=C) 1625 (m), *v*($SbF_6$) 656 (s).

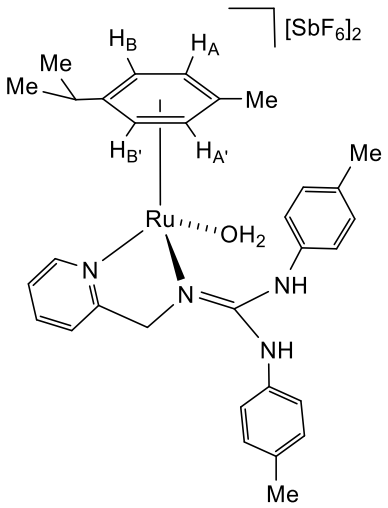


*R*$_{Ru}$-**5**

*R*$_{Ru}$-**5**. *$^1$H NMR (500.10 MHz, (CD$_3$)$_2$CO, 243K):* $\delta$ = 9.63 (d, *J* = 5.7 Hz, 1H, $H_6$Py), 9.18 (s, 1H, NH *trans* $CH_2$), 8.19 (t, *J* = 6.6 Hz, 1H, $H_4$Py), 7.88 (s, 1H, NH *trans* Ru), 7.77 (t, *J* = 7.8 Hz, 1H, $H_5$Py), 7.71 (d, *J* = 7.8 Hz, 1H, $H_3$Py), 7.54 (bs), 7.26 (d, *J* = 8.2 Hz), 7.17 (d, *J* = 8.2 Hz), 7.16 (bs) (8H, CH *p*-Tol), 6.45 (d, *J* = 6.2 Hz, 1H, $H_B$), 6.34 (d, *J* = 6.1 Hz, 1H, $H_{B'}$), 6.29 (d, 1H, $H_{A'}$), 6.13 (d, 1H, $H_A$), 5.08 (d, *J* = 18.8 Hz, 1H, $H_{pro\text{-}R}$ $CH_2$), 5.00 (d, 1H, $H_{pro\text{-}S}$ $CH_2$), 4.08 (bs, $H_2O$), 2.72 (spt, 1H, CH *i*Pr *p*-cymene), 2.27, 2.26 (2 × s, 9H, Me *p*-Tol, Me *p*-cymene), 1.19, 1.18 (2 × bd, *J* = 6.9 Hz, 6H, 2 × Me *i*Pr *p*-cymene).

*$^{13}$C{$^1$H} NMR (125.77 MHz, (CD$_3$)$_2$CO, 243K):* $\delta$ = 164.33 ($C_2$Py), 156.52 (C=N), 155.74 ($C_6$Py), 141.98 ($C_4$Py), 137.41, 137.28, 135.08, 134.69, 131.48, 131.17, 121.77 - 121.55, 119.95 (Ar *p*-Tol), 127.13 ($C_5$Py), 123.20 ($C_3$Py), 103.16 (C−*i*Pr *p*-cymene), 101.02 (C−Me *p*-cymene), 87.42 ($CH_B$), 86.18 ($CH_{A'}$), 85.35 ($CH_A$), 81.73 ($CH_{B'}$), 61.91 ($CH_2$), 32.26 (CH *i*Pr), 24.14, 21.40 (2 × Me *i*Pr *p*-cymene), 21.33, 21.30 (2 × Me *p*-Tol), 18.90 (Me *p*-cymene).

Complex **6**. Yield: 685.4 mg, 97 %. Anal. Calcd for $C_{39}H_{46}N_3F_{12}ORuPSb_2$: C, 39.8; H, 3.9; N, 3.6. Found: C, 39.4; H, 4.0; N, 3.4. HRMS ($\mu$-TOF), $C_{39}H_{46}N_3F_{12}ORuPSb_2$, [M-2$SbF_6$-$H_2O$-H]$^+$, calcd: 686.2243, found: 686.2256. IR (cm$^{-1}$): $\nu$(NH), $\nu$(OH) 3130-3430 (br), $\nu$(N=C) 1660 (w), $\nu$($SbF_6$) 654 (s).

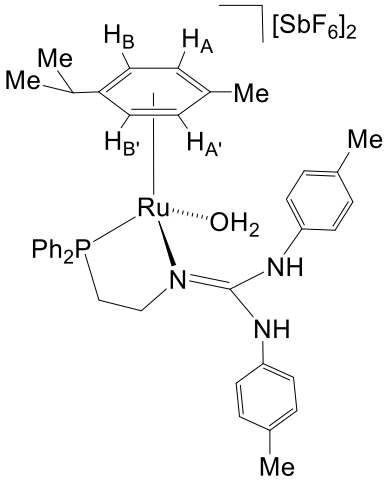


*R*$_{Ru}$-**6**

*R*$_{Ru}$-**6** enantiomer. *$^1$H NMR (500.10 MHz, $CD_2Cl_2$, RT)*: $\delta$ = 8.19 (bs, NH), 7.77 - 7.42 (m, 10H, $PPh_2$), 6.88, 6.76, 6.66, 6.10 (4 × bs, 8H, CH *p*-Tol), 6.50 (d, *J* = 6.3 Hz, 1H, $H_B$), 5.81 (d, 1H, $H_A$), 5.75 (d, *J* = 5.9 Hz, 1H, $H_{A'}$), 5.23 (bs, 1H, $H_{B'}$), 3.88 (bm, 1H, $H_{pro\text{-}R}$ $NCH_2$), 3.19 (m, 1H, $H_{pro\text{-}S}$ $NCH_2$), 3.09 (m, 1H, $H_{pro\text{-}R}$ $PCH_2$), 2.55 (m, 1H, $H_{pro\text{-}S}$ $PCH_2$), 2.41 (spt, 1H, CH *i*Pr *p*-cymene), 2.18, 2.16 (2 × s, 6H, Me *p*-Tol), 1.69 (s, 3H, Me *p*-cymene), 1.21 and 1.03 (2 × d, *J* = 7.0 Hz, 6H, 2 × Me *i*Pr *p*-cymene).

*$^{13}C\{^1H\}$ NMR (125.77 MHz, $CD_2Cl_2$, RT):* $\delta$ = 134.41 - 130.70 ($PPh_2$, Ar *p*-Tol), 124.88, 124.00 (Ar *p*-Tol), 102.20 (*C*−Me *p*-cymene), 112.05 (*C*−*i*Pr *p*-cymene), 92.98 ($CH_A$), 90.32 ($CH_B$), 88.85 ($CH_{B'}$), 85.88 ($CH_{A'}$), 53.35 ($CH_2N$), 31.73 (CH *i*Pr *p*-cymene), 25.08 (d, *J* = 28.7, $CH_2P$), 23.46, 22.84 (2 × Me *i*Pr *p*-cymene), 21.37 (2 × Me *p*-Tol), 18.18 (Me *p*-cymene).

*$^{31}P\{^1H\}$ NMR (202.46 MHz, $CD_2Cl_2$, RT):* $\delta$ = 54.12 (bs).

Complex **7**. Yield: 443.7 mg, 92 %. Anal. Calcd for $C_{42}H_{52}N_3F_{12}OPRuSb_2$: C, 41.4; H, 4.3; N, 3.4. Found: C, 41.9; H, 4.3; N, 3.5. HRMS ($\mu$-TOF), $C_{42}H_{52}N_3F_{12}OPRuSb_2$, [M-$H_2O$-H-2$SbF_6$], calcd: 728.2730, found: 728.2713. IR ($cm^{-1}$): $\nu$(NH) 3445 - 3130 (w), $\nu$(N=C) 1654 (w), $\nu$($SbF_6$) 654 (s).

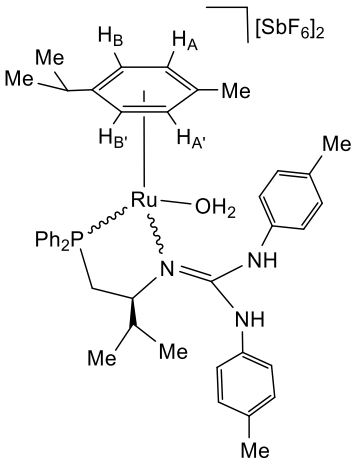


**7**

$R_{Ru}$,$S_C$-**7** diastereomer. *$^1$H NMR (500.10 MHz, $CD_2Cl_2$, RT):* $\delta$ = 7.88 - 7.46 (m, 10H, $PPh_2$), 6.85, 6.78, 6.51, 6.15 (4 × bs, 8H, CH *p*-Tol), 6.15 (d, *J* = 6.2 Hz, 1H, $H_B$), 6.05 (d, *J* = 5.9 Hz, 1H, $H_{A'}$), 5.89 (d, 1H, $H_{B'}$), 5.80 (d, 1H, $H_A$), 3.34 (m, 1H, C*H), 3.06, 2.82 (2 × m, 2H, $PCH_2$), 2.23 (spt, 1H, CH *i*Pr *p*-cymene)), 2.18, 2.16 (2 × s, 6H, Me *p*-Tol), 1.71 (s, 3H, Me *p*-cymene), 1.59 (m, 1H, CH *i*Pr **$H_2$L3**), 1.10 and 1.08 (2 × d, *J* = 6.7 Hz, 6H, 2 × Me *i*Pr *p*-cymene), 1.08 (d, *J* = 7.6 Hz, 6H, 2 × Me *i*Pr **$H_2$L3**).

*$^{13}$C{$^1$H} NMR (125.77 MHz, $CD_2Cl_2$, RT):* $\delta$ = 154.88 (C=N), 139.38 - 136.76, 130.59, 130.51, 124.10, 124.02 (Ar *p*-Tol), 134.41 - 126.60 ($PPh_2$), 115.11 (*C*-*i*Pr *p*-cymene), 102.21 (*C*–Me *p*-cymene), 90.72 ($CH_A$), 89.39 ($CH_{B'}$), 87.65 ($CH_{A'}$), 86.27 ($CH_B$), 67.85 (C*), 31.57 (CH *i*Pr *p*-cymene), 31.28 (s, CH *i*Pr **$H_2$L3**), 28.01 (d, *J* = 26.8 Hz, $CH_2P$), 22.82, 22.70 (2 × Me *i*Pr *p*-cymene), 21.26 (2 × Me *p*-Tol), 19.37 (2 × Me *i*Pr **$H_2$L3**), 18.46 (Me *p*-cymene).

*$^{31}$P{$^1$H} NMR (202.46 MHz, $CD_2Cl_2$, RT)*: $\delta$ = 53.49 (bs).

*$^{31}P\{^1H\}$ NMR (202.46 MHz, $CD_2Cl_2$, 193 K)*: $\delta$ = 56.05 (bs), 54.36 (bs).

$S_{Ru}$,$S_C$-**7** diastereomer. *$^1H$ NMR (500.10 MHz, $CD_2Cl_2$, RT):* $\delta$= 7.88 - 7.46 (m, 10H, $PPh_2$), 7.23 (s, 1H, NH), 7.17 (s, 1H, NH), 6.78, 6.61 (2 × d, *J* = 7.9 Hz, 4H, CH *p*-Tol), 6.71, 6.51 (2 × d, *J* = 8.4 Hz, 4H, CH *p*-Tol), 6.66 (d, *J* = 6.6 Hz, 1H, $H_B$), 5.96 (d, *J* = 6.0 Hz, 1H, $H_{A'}$), 5.85 (d, 1H, $H_A$), 4.79 (d, 1H, $H_{B'}$), 3.34, 2.55 (2 × m, 2H, $PCH_2$), 3.06 (m, 1H, C*H), 2.40 (m, 1H, CH *i*Pr **$H_2$L3**), 2.28 (sp, 1H, CH *i*Pr *p*-cymene), 2.10, 2.08 (2 × s, 6H, Me *p*-Tol), 1.52 (s, 3H, Me *p*-cymene), 1.46, 1.32 (2 × d, *J* = 6.6 Hz, 6H, 2 × Me *i*Pr **$H_2$L3**), 1.22, 0.96 (2 × d, *J* = 6.7 Hz, 6H, 2 × Me *i*Pr *p*-cymene).

*$^{13}C\{^1H\}$ NMR (125.77 MHz, $CD_2Cl_2$, RT):* $\delta$ = 149.85 (C=N), 139.38 - 136.76, 130.44, 130.07, 129.25, 125.06 (Ar *p*-Tol), 134.41 - 126.60 ($PPh_2$), 109.42 (*C*-*i*Pr *p*-cymene), 101.01 (*C*−Me *p*-cymene), 97.11 ($CH_A$), 91.38 ($CH_B$), 89.17 ($CH_{B'}$), 84.60 ($CH_{A'}$), 76.73 (C*), 33.24 (d, *J* = 12.1 Hz, CH *i*Pr **$H_2$L3**), 31.89 (CH *i*Pr *p*-cymene), 26.10 (d, *J* = 29.5 Hz, $CH_2P$), 23.29, 22.87 (2 × Me *i*Pr *p*-cymene), 22.91, 20.75 (2 × Me *i*Pr **$H_2$L3**), 21.37, 21.34 (2 × Me *p*-Tol), 17.50 (Me *p*-cymene).

*$^{31}P\{^1H\}$ NMR (202.46 MHz, $CD_2Cl_2$, RT)*: $\delta$ = 43.69 (bs).

*Preparation of the complexes [($\eta^6$-p-cymene)Ru(**HL**)][$SbF_6$] (**$H_2$L** = **$H_2$L1 (8)**, **$H_2$L2 (9)**, **$H_2$L3 (10)**)*

Under argon, $NaHCO_3$ (30.0 mg, 0.33 mmol) was added to complex **5**, **6** or **7** (0.33 mmol) in methanol (10 mL) and the mixture stirred for *ca*. 1 day. The resulting suspension was filtered and vacuum-evaporated until dryness. The residue was extracted with dichloromethane (3 × 10 mL) and the resulting solution was concentrate under reduced pressure to *ca*. 2mL. Slow addition of *n*-pentane (10 mL) resulted in the precipitation of an orange (complex **8**) or yellow (complexes **9** and **10**) solid which was washed with *n*-

pentane (2 × 10 mL) and vacuum-evaporated until dryness. Single-crystals were developed by slow evaporation of 2-propanol solutions (**9**) or from $Et_2O$/MeOH solutions (**10**).

Complex **8**. Yield: 278.1 mg, 94 %. Anal. Calcd for $C_{31}H_{35}N_4F_6RuSb \cdot 1/2CH_2Cl_2$: C, 44.9; H, 4.3; N, 6.7. Found: C, 44.9; H, 4.3; N, 6.7. HRMS ($\mu$-TOF), $C_{31}H_{35}N_4F_6RuSb$, $[M\text{-}SbF_6]^+$, calcd: 565.1908, found: 565.1926. IR ($cm^{-1}$): $\nu$(NH) 3358 (br), $\nu$(N=C) 1629 (m), $\nu(SbF_6)$ 654 (s).

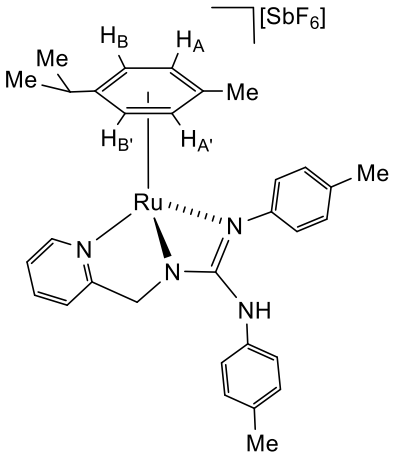


$R_{Ru}S_N$-**8**

$R_{Ru,}S_N$-**8** diastereomer. *$^1$H NMR (500.10 MHz, $CD_2Cl_2$, RT)*: $\delta$ = 9.32 (d, $J$ = 5.3 Hz, 1H, $H_6$Py), 7.83 (t, $J$ = 7.6 Hz, 1H, $H_4$Py), 7.49 (t, $J$ = 6.4 Hz, 1H, $H_5$Py), 7.21 (d, $J$ = 7.6 Hz, 1H, $H_3$Py), 7.14 (d, $J$ = 8.1 Hz), 7.11 (d, $J$ = 8.1 Hz), 6.94 (d), 6.90 (d) (8H, CH *p*-Tol), 5.87 (bs, 1H, NH), 5.71 (m, 2H, $H_{B,}$ $H_{B'}$), 5.56 (bd, $J$ = 5.2 Hz, 2H, $H_A$, $H_{A'}$), 4.20 (d, $J$ = 17.4 Hz, 1H, $H_{pro\text{-}S}$ $CH_2$), 4.09 (d, 1H, $H_{pro\text{-}R}$ $CH_2$), 2.50 (spt, 1H, CH *i*Pr *p*-cymene)), 2.31, 2.30 (s, 6H, Me *p*-Tol), 1.99 (s, 3H, Me *p*-cymene), 1.19 and 1.13 (2 × d, $J$ = 6.9 Hz, 6H, 2 × Me *i*Pr *p*-cymene).

*$^{13}C\{^1H\}$ NMR (125.77 MHz, $CD_2Cl_2$, RT)*: $\delta$ = 165.92 ($C_2$ Py), 165.39 (C=N), 155.37 ($C_6$ Py), 140.21 ($C_4$ Py), 131.13, 130.94, 123.28 (Ar *p*-Tol), 125.53 ($C_5$ Py), 122.79 ($C_3$ Py), 103.10 (*C*−Me *p*-cymene), 98.94 (*C*−*i*Pr *p*-cymene), 84.05, 83.86 ($CH_B$, $CH_{B'}$), 82.98,

82.95 ($CH_A$, $CH_{A'}$), 59.43 ($CH_2$), 32.07 (CH *i*Pr), 23.17, 22.75 (2 × Me *i*Pr), 21.41, 21.30 (2 × Me *p*-Tol), 19.16 (Me *p*-cymene).

Complex **9**. Yield: 283.0 mg, 93 %. Anal. Calcd for $C_{39}H_{43}N_3F_6PRuSb$: C, 50.8; H, 4.7; N, 4.6. Found: C, 50.6; H, 4.8; N, 4.6. HRMS ($\mu$-TOF), $C_{39}H_{43}N_3F_6PRuSb$, $[M\text{-}SbF_6]^+$, calcd: 686.2243, found: 686.2254 IR ($cm^{-1}$): $\nu$(NH) 3368 (w), $\nu$(N=C) 1593 (w), $\nu(SbF_6)$ 654 (s).

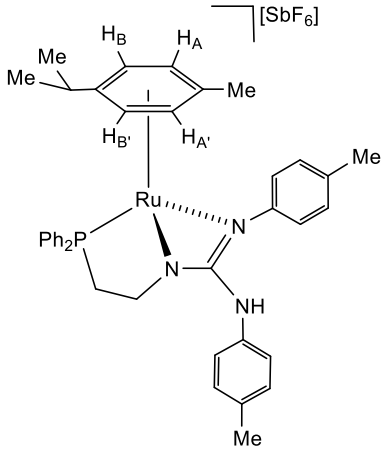


$R_{Ru}$,$S_N$-**9**

$R_{Ru}$,$S_N$-**9** diastereomer. *$^1$H NMR (500.10 MHz, $CD_2Cl_2$, RT)*: $\delta$ = 7.76 - 7.30 (m, 10H, $PPh_2$), 7.09, 6.71 (2 × d, *J* = 8.1 Hz) (4H, CH *p*-Tol), 7.05, 6.81 (2 × d, *J* = 8.2 Hz) (4H, CH *p*-Tol), 5.83 (s, 1H, NH), 5.48 (d, *J* = 5.9 Hz, 1H, $H_B$), 5.25 (d, 1H, $H_A$), 5.09 (d, *J* = 5.8 Hz, 1H, $H_{B'}$), 4.85 (d, 1H, $H_{A'}$), 3.46 (dm, *J* = 34.8 Hz, 1H, $H_{pro\text{-}R}$ $NCH_2$), 3.08 (m, 1H, $H_{pro\text{-}S}$ $NCH_2$), 2.76 (spt, 1H, CH *i*Pr *p*-cymene), 2.70 (m, 1H, $H_{pro\text{-}R}$ $PCH_2$), 2.59 (m, 1H, $H_{pro\text{-}S}$ $PCH_2$), 2.31, 2.29 (2 × s, 6H, Me *p*-Tol), 2.14 (s, 3H, Me *p*-cymene) and 1.37 and 1.31 (2 × d, *J* = 6.9 Hz, 6H, 2 × Me *i*Pr *p*-cymene).

*$^{13}C\{^1H\}$ NMR (125.77 MHz, $CD_2Cl_2$, RT)*: $\delta$ = 161.90 (C=N), 134.89 - 129.98 ($PPh_2$), 130.99, 130.74, 123.31, 119.79 (Ar *p*-Tol), 112.03 (*C*−*i*Pr *p*-cymene), 101.34 (*C*−Me *p*-cymene), 88.95 ($CH_B$), 88.48 ($CH_{A'}$), 87.98 ($CH_A$), 84.21 ($CH_{B'}$), 52.37 ($CH_2N$), 33.85

($CH_2P$), 32.52 (CH *i*Pr *p*-cymene), 23.93, 22.59 (2 × Me *i*Pr *p*-cymene), 21.34, 21.24 (2 × Me *p*-Tol), 19.37 (Me *p*-cymene).

*$^{31}P\{^1H\}$ NMR (202.46 MHz, $CD_2Cl_2$, RT)*: $\delta$ = 55.93 (s).

Complex **10**. Yield: 301.9 mg, 95%. Anal. Calcd for $C_{42}H_{49}N_3F_6PRuSb$: C, 52.4; H, 5.1; N, 4.4. Found: C, 53.2; H, 5.4; N, 4.4. HRMS ($\mu$-TOF), $C_{42}H_{49}N_3F_6PRuSb$, $[M\text{-}SbF_6]^+$, calcd: 728.2713, found: 728.2729. IR ($cm^{-1}$): *v*(NH) 3379 (w), *v*(N=C) 1593 (w), *v*($SbF_6$) 655 (s).

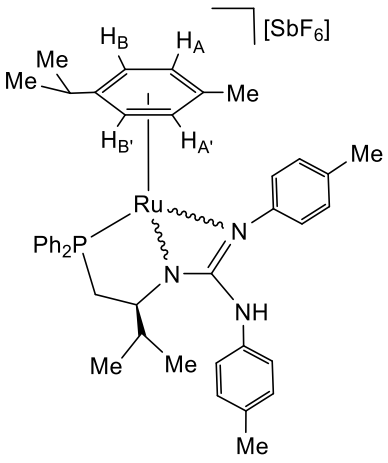


**10**

*$R_{Ru}$,$S_N$,$S_C$*-**10** diastereomer. *$^1H$ NMR (500.10 MHz, $CD_2Cl_2$, RT)*: $\delta$= 7.80 - 7.36 (m, 10H, $PPh_2$), 6.94, 6.70 (2 × d, *J* = 8.2 Hz, 4H, CH *p*-Tol), 6.74, 6.05 (2 × d, *J* = 8.0 Hz, 4H, CH *p*-Tol), 5.71 (s, 1H, NH), 5.43 (d, *J* = 6.0 Hz, 1H, $H_B$), 5.38 (d, *J* = 5.9 Hz, 1H, $H_{A'}$), 5.18 (d, 1H, $H_{B'}$), 4.70 (d, 1H, $H_A$), 3.17 (m, 1H, $H_{pro\text{-}S}$ $PCH_2$), 3.00 (m, 1H, C*H), 2.74 (m, 1H, $H_{pro\text{-}R}$ $PCH_2$), 2.55 (spt, 1H, CH *i*Pr *p*-cymene), 2.22, 2.15 (2 × s, 6H, Me *p*-Tol), 1.92 (s, 3H, Me *p*-cymene), 1.73 (m, 1H, CH *i*Pr **HL3**), 1.28 and 1.22 (2 × d, *J* = 7.0 Hz, 6H, 2 × Me *i*Pr *p*-cymene), 1.24, 1.07 (2 × d, *J* = 6.6 Hz, 6H, 2 × Me *i*Pr **HL3**).

*$^{13}C\{^1H\}$ NMR (125.77 MHz, $CD_2Cl_2$, RT): $\delta$* = 159.96 (C=N), 144.50, 135.32, 134.18, 133.92, 130.42, 130.11, 121.90, 120.14 (Ar *p*-Tol), 134.74 – 128.63 ($PPh_2$), 114.40 (C-*i*Pr *p*-cymene), 103.55 (*C*-Me *p*-cymene)), 88.74 ($CH_B$), 86.94 ($CH_{A'}$), 84.74 ($CH_A$),

83.59 ($CH_{B'}$), 63.58 (C*), 40.55 (d, $J$ = 35.1 Hz, $CH_2P$), 35.70 (d, $J$ = 4.3 Hz, CH *i*Pr **HL3**), 32.34 (CH *i*Pr *p*-cymene), 24.48, 22.50 (2 × Me *i*Pr *p*-cymene), 21.77, 19.63 (2 × Me *i*Pr **HL3**), 21.25, 21.12 (2 × Me *p*-Tol), 19.40 (Me *p*-cymene).

*$^{31}P\{^1H\}$ NMR (202.46 MHz, $CD_2Cl_2$, RT)*: $\delta$ = 49.65 (s).

$S_{Ru}$,$R_N$,$S_C$-**10** diastereomer. *$^1H$ NMR (500.10 MHz, $CD_2Cl_2$, RT)*: $\delta$= 7.90 - 7.10 (m, 10H, $PPh_2$), 6.82, 6.68 (2 × d, $J$ = 8.3 Hz), 6.46, 5.83 (2 × d, $J$ = 8.3 Hz) (8H, CH *p*-Tol) 5.81 (s, 1H, NH), 5.55 (m, 2H, $H_A$, $H_B$), 5.11, 4.53 (2 × d, $J$ = 6.4 Hz, 2H, $H_{A'}$, $H_{B'}$), 2.33, 2.17, 2.02 (3 × s, 9H, Me *p*-Tol, Me *p*-cymene), 1.46 (d, $J$ = 6.6 Hz, 3H), 1.14 (d, $J$ = 6.1 Hz, 3H) (2 × Me *i*Pr *p*-cymene or 2 × Me *i*Pr **HL3**).

*$^{31}P\{^1H\}$ NMR (202.46 MHz, $CD_2Cl_2$, RT)*: $\delta$ = 48.98 (s).

**X-ray crystallography**

X-ray diffraction data were collected on a Smart APEX (complex **1**, **9** and **10**) or APEX DUO (complexes **2** and **5**) Bruker diffractometers, using graphite-monochromated Mo κα radiation (λ=0.71073 Å). Selected crystals were mounted on a fiber, coated with a protecting perfluoropolyether oil and cooled to 100(2) K with an open-flow nitrogen gas. Data were collected using ω-scans with narrow oscillation frame strategy (Δω = 0.3°). Data were integrated and corrected from absorption effects with SAINT[50] and SADABS[51] programs, included in APEX3 package. Crystal structures were solved by direct methods with SHELXS-2013 and refined by full-matrix least squares on $F^2$ with SHELXL program[52-54] included in Wingx program system.[55] Disordered solvent region in complex **1** has been analysed with SQUEEZE program.[56] Most of the hydrogen atoms have been included in the model in calculated positions and refined with a riding model. Those of N−H have been included in observed positions. Geometrical restraints

concerning N−H bond lengths have been used in refinement of complexes **1**, **2** and **5** structural models. Special details about refinement restraints or disorder are commented below.

**Crystal data for complex 1**: $C_{31}H_{36}ClF_6N_4RuSb \cdot 1.5(CH_4O)$; $M_r$ = 884.97; orange plate, 0.080 × 0.120 × 0.240 mm$^3$; triclinic $P\bar{1}$; $a$ = 10.8473(7) Å, $b$ = 11.2302(7) Å, $c$ = 15.2419(10) Å, α= 91.9498(8) °, $\beta$ = 93.0010(10) °, γ= 110.6124(8) °; $V$ = 1730.39(19) Å$^3$, $Z$ = 2, $D_c$= 1.677 g/cm$^3$; $\mu$= 1.358 cm$^{-1}$; min. and max. absorption correction factors: 0.7432 and 0.8621; $2\theta_{max}$=56.796°; 16029 reflections measured, 8121 unique; $R_{int}$ = 0.0221; number of data/restraint/parameters 8121/1/410; $R_1$= 0.0361 [6736 reflections, $I > 2\sigma(I)$], w$R(F^2)$ = 0.0872 (all data); largest difference peak 1.146 e·Å$^{-3}$.

**Crystal data for complex 2**: $2(C_{39}H_{44}ClF_6N_3PRuSb) \cdot CH_4O$; $M_r$ = 1948.06; red prism, 0.180 × 0.200 × 0.300 mm$^3$; monoclinic $P2_1/c$; $a$ = 30.2375(14) Å, $b$ = 11.5147(6) Å, $c$ = 25.2041(12) Å, $\beta$ = 112.8070(10) °; $V$ = 8089.4(7) Å$^3$, $Z$ = 4, $D_c$ = 1.600 g/cm$^3$; $\mu$ = 1.208 cm$^{-1}$; min. and max. absorption correction factors: 0.7463 and 0.8132; $2\theta_{max}$ = 56.826 °; 150927 reflections measured, 20210 unique; $R_{int}$ = 0.0365; number of data/restraint/parameters 20210/5/985; $R_1$ = 0.0265[17361 reflections, $I > 2\sigma(I)$], w$R(F^2)$ = 0.0613 (all data); largest difference peak 1.480 e·Å$^{-3}$.

**Crystal data for complex 5**: $C_{31}H_{38}F_{12}N_4ORuSb_2 \cdot 2(CH_2Cl_2)$; $M_r$ = 1225.07; red prism, 0.180 × 0.200 × 0.300 mm$^3$; triclinic $P\bar{1}$; $a$ = 8.8333(7) Å, $b$ = 15.2675(11) Å, $c$ = 17.5928(13) Å, α = 110.3530(10) °, $\beta$ = 92.9260(10) °, γ = 98.3460(10) °, $Z$ = 2, $D_c$ = 1.860 g/cm$^3$; $\mu$ = 1.895 cm$^{-1}$; min. and max. absorption correction factors: 0.6324 and 0.8371; $2\theta_{max}$ =52.864°; 29876 reflections measured, 8887 unique; $R_{int}$ = 0.0596; number of data/restraint/parameters 8887/0/521; $R_1$ = 0.0828[6131 reflections, $I > 2\sigma(I)$], w$R(F^2)$ = 0.2455 (all data); largest difference peak 3.724 e.Å$^{-3}$. Hydrogen atoms of coordinated water of complex **5** have not been observed in Fourier difference maps. HFIX 137

instruction has been used to calculate three possible positions. Afterwards, their isotropic atomic displacement parameters have been refined. The obtained $U_{iso}$ values have been used as criteria to select the two most suitable positions. The positions have been fixed and the Uiso have been restrained. Fluorine atoms of one of the counterions have been found to be disordered. They have been included in the model in two sets of positions and isotropically refined with complementary occupancy factors (0.52/0.48(2)).

**Crystal data for complex 9**: $C_{39}H_{43}F_6N_3PRuSb \cdot C_3H_8O$; $M_r$ = 981.64; yellow plate, 0.100 × 0.105 × 0.165 mm$^3$; orthorhombic *Pna*2$_1$; $a$ = 25.0911(15) Å, $b$ = 10.2270(6) Å, $c$ = 16.2844(10) Å °; $V$ = 4178.7(4) Å$^3$, $Z$ = 4, $D_c$ = 1.560 g/cm$^3$; $\mu$ = 1.109 cm$^{-1}$; min. and max. absorption correction factors: 0.8042 and 0.9010; $2\theta_{max}$ =56.672 °; 64971 reflections measured, 10311 unique; $R_{int}$ = 0.0579; number of data/restraint/parameters 10311/1/511; $R_1$ = 0.0389 [9227 reflections, $I > 2\sigma(I)$], w$R(F^2)$ = 0.0925 (all data); largest difference peak 0.761 e·Å$^{-3}$. Flack parameter: -0.035(10). Carbon and hydrogen atoms of the solvent have been found to be disordered. They have been included in the model in two sets of positions and isotropically refined with complementary occupancy factors (0.61/0.39(2)).

**Crystal data for complex 10**: $C_{42}H_{49}F_6N_3PRuSb \cdot 2(C_4H_{10}O)$; $M_r$ = 1111.87; yellow plate, 0.125 × 0.225 × 0.320 mm$^3$; orthorhombic $P2_12_12_1$; $a$ = 11.1095(6) Å, $b$ = 13.4487(7) Å, $c$ = 33.9251(18) Å; $V$ = 5068.7(5) Å$^3$, $Z$ = 4, $D_c$ = 1.457 g/cm$^3$; $\mu$ = 0.925 cm$^{-1}$; min. and max. absorption correction factors: 0.7748 and 0.8621; $2\theta_{max}$ = 58.040 °; 74534 reflections measured, 12771 unique; $R_{int}$ = 0.0276; number of data/restraint/parameters 12771/0/596; $R_1$ = 0.0398 [12456 reflections, $I > 2\sigma(I)$], w$R(F^2)$ = 0.0855 (all data); largest difference peak 1.042 e·Å$^{-3}$; Flack parameter: -0.002(4).

**Computational details**

DFT geometry optimizations and thermochemical calculations were carried out with the Gaussian 09 program package,[57] using the B3LYP-D3 hybrid functional.[58-61] Geometry optimizations were performed in the gas phase with the LanL2TZ(f) effective core potential basis set for the ruthenium atoms, and the 6-311G(d,p) basis set for the remaining ones. All minima (no imaginary frequencies) and transition states (one imaginary frequency) were characterized by calculating the Hessian matrix. ZPE and gas-phase thermal corrections (entropy and enthalpy, 298.15 K, 1 atm) from these analyses were calculated. The nature of the transition states was confirmed by IRC calculations.

## Supplementary Material

Electronic supporting information available: NMR spectra or the compounds. Supporting information for this article is available on the WWW under https://doi.org/ ……..

CCDC 2070481-2070485 contains the supplementary crystallographic data for this paper. These data can be obtained free of charge from The Cambridge Crystallographic Data Centre via www.ccdc.cam.ac.uk/structures.

## Author Contributions Statement

E.-T. W. carried out the experiments, F. V. performed the characterization through NMR spectroscopy, J. A. L. carried out the DFT studies, P. G.-O. and F. J. L. performed the X-ray structural studies, R. R. designed the experiments and interpreted the results, P. L. and D. C. designed the project, interpreted the results and wrote the manuscript.

## Acknowledgements

We thank the Ministerio de Ciencia Innovación y Universidades of Spain (CTQ2018-095561-BI00 and CTQ2017-83421-P) and Gobierno de Aragón (Grupo Consolidado: Catalizadores Organometálicos Enantioselectivos) for financial support. R. R. acknowledges the Ministerio de Economía y Competitividad of Spain for a Ramón y Cajal (RYC-2013-13800) grant. P. G.-O. acknowledges CSIC for finantial support under a PIE project.

## References

[1] J. Francos, V. Cadierno, "The chemistry of guanidinate complexes of the platinum group metals", *Dalton Trans.* **2019**, *48*, 9021-9036.

[2] T. Chlupatý, A. Ruzicka, "Hybrid amidinates and guanidinates of main group metals", *Coord. Chem. Rev.* **2016**, *314*, 103-113.

[3] Themed issue: *The Chemistry of Guanidine, Guanidinium, and Guanidinate Compounds*, *Aust. J. Chem.*, 2014, Vol. 67(7), https://www.publish.csiro.au/CH/issue/6955.

[4] F. T. Edelmann, "Recent Progress in the Chemistry of Metal Amidinates and Guanidinates: Syntheses, Catalysis and Materials", *Adv. Organomet. Chem*. **2013**, *61*, 55-374.

[5] A. A. Trifonov, "Guanidinate and amidopyridinate rare-earth complexes: Towards highly reactive alkyl and hydrido species", *Coord. Chem. Rev*. **2010**, *254*, 1327-1347.

[6] C. Jones, “Bulky guanidinates for the stabilization of low oxidation state metallacycles”, *Coord. Chem. Rev*. **2010**, *254*, 1273-1289.

[7] M. P. Coles, “Bicyclic-guanidines, -guanidinates and -guanidinium salts: wide ranging applications from a simple family of molecules”, *Chem. Commun*. **2009**, 3659-3676.

[8] F. T. Edelmann, “Advances in the Coordination Chemistry of Amidinate and Guanidinate Ligands”, *Adv. Organomet. Chem*. **2008**, *57*, 183-352.

[9] M. P. Coles, “Application of neutral amidines and guanidines in coordination chemistry”, *Dalton Trans*. **2006**, 985-1001

[10] P. J. Bailey, S. Pace, “The coordination chemistry of guanidines and guanidinates”, *Coord. Chem. Rev*. **2001**, *214*, 91-141.

[11] X.-Y. Cui, C.-H. Tan, D. Leow, “Metal-catalysed reactions enabled by guanidine-type Ligands”, *Org. Biomol. Chem*. **2019**, *17*, 4689-4699.

[12] Topics in Heterocyclic Chemistry, *Guanidines as Reagents and Catalysts I and II*, ed. P. Selig, Springer, Cham, Switzerland, **2017**.

[13] F. T. Edelmann, “Lanthanide amidinates and guanidinates in catalysis and materials science: a continuing success story”, *Chem. Soc. Rev*. **2012**, *41*, 7657-7672.

[14] S. Collins, “Polymerization catalysis with transition metal amidinate and related complexes”, *Coord. Chem. Rev*. **2011**, *255*, 118-138.

[15] F. T. Edelmann, “Lanthanide amidinates and guanidinates: from laboratory curiosities to efficient homogeneous catalysts and precursors for rare-earth oxide thin films”, *Chem. Soc. Rev*. **2009**, *38*, 2253-2268.

[16] M. K. Kiesewetter, E. J. Shin, J. L. Hedrick, R. M. Waymouth, "Organocatalysis: Opportunities and Challenges for Polymer Synthesis", *Macromolecules* **2010**, *43*, 2093-2107 and references therein.

[17] R. G. S. Berlinck, S. Romminger, "The chemistry and biology of guanidine natural products", *Nat. Prod. Rep*. **2016**, *33*, 456-490 and references therein.

[18] P. Blondeau, M. Segura, R. Pérez-Fernández, J. de Mendoza, "Molecular recognition of oxoanions based on guanidinium receptors", *Chem. Soc. Rev*. **2007**, *36*, 198-210 and references therein.

[19] J. S. J. McCahill, G. C. Welch, D. W. Stephan, "Reactivity of "Frustrated Lewis Pairs": Three-Component Reactions of Phosphines, a Borane, and Olefins", *Angew. Chem. Int. Ed*. **2007**, *46*, 4968-4971.

[20] J. Lam, K. M. Szkop, E. Mosaferi, D. W. Stephan, "FLP catalysis: main group hydrogenations of organic unsaturated substrates", *Chem. Soc. Rev*. **2019**, *48*, 3592-3612.

[21] M.-A. Légaré, C. Pranckevicius, H. Braunschweig, "Metallomimetic Chemistry of Boron", *Chem. Rev*. **2019**, *119*, 8231-8261.

[22] A. R. Jupp, D. W. Stephan, "New Directions for Frustrated Lewis Pair Chemistry", *Trends Chem*. **2019**, *1*, 35-48.

[23] J. Paradies, "From structure to novel reactivity in frustrated Lewis pairs", *Coord. Chem. Rev*. **2019**, *380*, 170-183.

[24] F.-G. Fontaine É. Rochette, "Ambiphilic Molecules: From Organometallic Curiosity to Metal-Free Catalysts", *Acc. Chem. Res*. **2018**, *51*, 454-464.

[25] D. J. Scott, M. J. Fuchter, A. E. Ashley, "Designing effective 'frustrated Lewis pair'hydrogenation catalysts", *Chem. Soc. Rev*. **2017**, *46*, 5689-5700.

[26] D. W. Stephan, "The broadening reach of frustrated Lewis pair chemistry", *Science* **2016**, *354*, aaf7229.

[27] D. W. Stephan, "Frustrated Lewis Pairs", *J. Am. Chem. Soc*. **2015**, *137*, 10018-10032.

[28] D. W. Stephan, G. Erker, "Frustrated Lewis Pair Chemistry: Development and Perspectives", *Angew. Chem. Int. Ed*. **2015**, *54*, 6400-6441.

[29] D. W. Stephan, "Frustrated Lewis Pairs: From Concept to Catalysis", *Acc. Chem. Res*. **2015**, *48*, 306-316.

[30] D. W. Stephan, G. *Erker*, "Frustrated Lewis Pairs II: Expanding the Scope", *Top. Curr. Chem.* **2013**, *334*.

[31] D. W. Stephan, G. Erker, "Frustrated Lewis Pairs I: Uncovering and Understanding", *Top. Curr. Chem*. **2013**, 332.

[32] D. W. Stephan, G. Erker, "Frustrated Lewis Pairs: Metal-free Hydrogen Activation and More", *Angew. Chem. Int. Ed*. **2010**, *49*, 46-76.

[33] S. R. Flynn, D. F. Wass, "Transition Metal Frustrated Lewis Pairs", *ACS Catal*. **2013**, *3*, 2574-2581.

[34] Z. Jian, C. G. Daniliuc, G. Kehra, G. Erker, "Frustrated Lewis Pair vs Metal−Carbon σ- Bond Insertion Chemistry at an *o*- Phenylene-Bridged $Cp_2Zr^+/PPh_2$ System", *Organometallics* **2017**, *36*, 424-434 and references therein.

[35] N. Zwettler, N. C. Mösch-Zanetti, "Interaction of Metal Oxido Compounds with $B(C_6F_5)_3$", *Chem. Eur. J*. **2019**, *25*, 6064-6076.

[36] R. M. Bullock, G. M. Chambers, "Frustration across the periodic table: heterolytic cleavage of dihydrogen by metal complexes", *Phil. Trans. R. Soc. A* **2017**, *375*: 2017.0002.

[37] S. Arndt, M. Rudolph, A. S. K. Hashmi, "Gold-based frustrated Lewis acid/base pairs (FLPs)", *Gold Bull.* **2017**, *50*, 267-282.

[38] T. A. Rokob, A. Hamza, A. Stirling, I. Papai, "On the Mechanism of $B(C_6F_5)_3$-Catalyzed Direct Hydrogenation of Imines: Inherent and Thermally Induced Frustration", *J. Am Chem. Soc*. **2009**, *131*, 2029-2036.

[39] S. Roters, C. Appelt, H. Westenberg, A. Hepp, J. C. Slootweg, K. Lammertsma, W. Uhl, "Dimeric aluminum–phosphorus compounds as masked frustrated Lewis pairs for small molecule activation", *Dalton Trans.* **2012**, *41*, 9033-9045.

[40] M. Boudjelel, E. D. Sosa Carrizo, S. Mallet-Ladeira, S. Massou, K. Miqueu, G. Bouhadir, D. Bourissou, "Catalytic Dehydrogenation of (Di)Amine-Boranes with a Geometrically Constrained Phosphine-Borane Lewis Pair", *ACS Catal*. **2018**, *8*, 4459-4464.

[41] M. Carmona, J. Ferrer, R. Rodríguez, V. Passarelli, F. J. Lahoz, P. García-Orduña, L. Cañadillas-Delgado, D. Carmona, "Reversible Activation of Water by an Air and Moisture Stable Frustrated Rhodium Nitrogen Lewis Pair", *Chem. Eur. J*. **2019**, *25*, 13665-13670.

[42] A. Parker, P. Lamata, F. Viguri, R. Rodríguez, J. A. López, F. J. Lahoz, P. García-Orduña, D. Carmona, "Half-sandwich complexes of osmium containing guanidine-derived ligands", *Dalton Trans*. **2020**, 13601-13617.

[43] Á. Ávila, R. Chinchilla, E. Gómez-Bengoa, C. Nájera, "Enantioselective Synthesis of Succinimides by Michael Addition of Aldehydesto Maleimides Organocatalyzed by Chiral Primary Amine-Guanidines", *Eur. J. Org. Chem.* **2013**, 5085-5092.

[44] M. A. Bennet, T. N. Huang, T. W. Matheson, A. K. Smith, "$\eta^6$-(Hexamethylbenzene)ruthenium complexes: di-$\mu$-chloro-bis[chloro($\eta^6$-1-isopropyl-4-methyl-benzene)ruthenium(II)]", *Inorg. Synth*. **1982**, *21*, 75.

[45] C. Lecomte, Y. Dusausoy, J. Protas, J. Tirouflet, "Structure cristalline et configuration relative d'un complexe du titanocene presentant une chiralite plane et une chiralite centree sur l'atome de titane", *J. Organomet. Chem*. **1974**, *73*, 67-76.

[46] J. Bernstein, E. Davis, L. Shimoni, N.-L. Chang "Patterns in Hydrogen bonding: Functionality and Graph Set Analysis in Crystals", *Angew. Chem. Int. Ed. Eng*. **1995**, *34*, 1555-1573.

[47] Small amounts of other two compounds were also detected. Most probably, one of them is an oxide of the **$H_2$L3** ligand (7 %, $\delta$P($CD_2Cl_2$) = 34.70 ppm, HRMS ($\mu$-TOF), $C_{32}H_{36}N_3OP$, $[M + H]^+$, calcd: 510.2669, found: 510.2673). The structure of the other compound (4 %) was not elucidated.

[48] *Dynamic NMR Spectroscopy*, ed. J. Sandstrom, Academic Press, London, 1982.

[49] M. L. H. Green, L. L. Wong, A. Sella, "Relationship between intramolecular chemical exchange and NMR-observed rate constants", *Organometallics* **1992**, *11*, 2660-2668.

[50] SAINT+, version 6.01: Area-Detector Integration Software, Bruker AXS, Madison 2001.

[51] SADABS 2016/02. L. Krause, R. Herbst-Irmer, G. M. Sheldrick, D. Stalke, "Comparison of silver and molybdenum microfocus X-ray sources for single-crystal structure determination", *J. Appl. Crystallogr*. **2015**, *48*, 3-10.

[52] G. M. Sheldrick, "Phase annealing in SHELX-90: direct methods for larger structures", *Acta Crystallogr*. *A* **1990**, *46*, 467-473.

[53] G. M. Sheldrick, "A short history of SHELX", *Acta Crystallogr*. *A* **2008**, *64*, 112-122.

[54] G. M. Sheldrick, "Crystal structure refinement with SHELXL", *Acta Crystallogr*. *C* **2015**, *71*, 3-8.

[55] L. J. Farrugia, "WinGX and ORTEP for *Windows*: an update", *J. Appl. Crystallogr*. **2012**, *45*, 849-854.

[56] A. L. Spek, *"PLATON SQUEEZE*: a tool for the calculation of the disordered solvent contribution to the calculated structure factors", *Acta Crystallogr*. **2015**, *C71*, 9-18.

[57] M. J. Frisch, G. W. Trucks, H. B. Schlegel, G. E. Scuseria, M. A. Robb, J. R. Cheeseman, G. Scalmani, V. Barone, B. Mennucci, G. A. Petersson, H. Nakatsuji, M. Caricato, X. Li, H. P. Hratchian, A. F. Izmaylov, J. Bloino, G. Zheng, J. L. Sonnenberg, M. Hada, M. Ehara, K. Toyota, R. Fukuda, J. Hasegawa, M. Ishida, T. Nakajima, Y. Honda, O. Kitao, H. Nakai, T. Vreven, J. A. Montgomery, Jr., J. E. Peralta, F. Ogliaro, M. Bearpark, J. J. Heyd, E. Brothers, K. N. Kudin, V. N. Staroverov, R. Kobayashi, J. Normand, K. Raghavachari, A. Rendell, J. C. Burant, S. S. Iyengar, J. Tomasi, M. Cossi, N. Rega, J. M. Millam, M. Klene, J. E. Knox, J. B. Cross, V. Bakken, C. Adamo, J. Jaramillo, R. Gomperts, R. E. Stratmann, O. Yazyev, A. J. Austin, R. Cammi, C. Pomelli, J. W. Ochterski, R. L. Martin, K.

Morokuma, V. G. Zakrzewski, G. A. Voth, P. Salvador, J. J. Dannenberg, S. Dapprich, A. D. Daniels, Ö. Farkas, J. B. Foresman, J. V. Ortiz, J. Cioslowski, and D. J. Fox, Gaussian 09, Revision D.01, Gaussian, Inc., Wallingford CT, 2011.

[58] C. Lee, W. Yang, R. G. Parr, "Development of the Colle-Salvetti correlation-energy formula into a functional of the electron density", *Phys. Rev. B* **1988**, ***37***, 785-789.

[59] A. D. Becke, "A new mixing of Hartree–Fock and local density- functional theories", *J. Chem. Phys*. **1993**, *98*, 1372-1377.

[60] A. D. Becke, "Density- functional thermochemistry. III. The role of exact exchange", *J. Chem. Phys*. **1993**, *98*, 5648-5652.

[61] S. Grimme, J. Antony, S. Ehrlich, H. Krieg, "A consistent and accurate ab initio parametrization of density functional dispersion correction (DFT-D) for the 94 elements H-Pu", *J. Chem. Phys*. **2010**, *132*, 154104.